Journal of Proteomics 273 (2023) 104795

Contents lists available at ScienceDirect

Journal of Proteomics

journal homepage: www.elsevier.com/locate/jprot

Diet and phytogenic supplementation substantially modulate the salivary proteome in dairy cows

Ezequias Castillo-Lopez [a,*,1], Cátia Pacífico [a,1,2], Arife Sener-Aydemir [a], Karin Hummel [b], Katharina Nöbauer [b], Sara Ricci [a], Raul Rivera-Chacon [a], Nicole Reisinger [c], Ebrahim Razzazi-Fazeli [b], Qendrim Zebeli [a], Susanne Kreuzer-Redmer [d,*]

[a] University of Veterinary Medicine Vienna, Institute of Animal Nutrition and Functional Plant Compounds, Christian Doppler Laboratory for Innovative Gut Health Concepts of Livestock, Vienna, Austria
[b] University of Veterinary Medicine Vienna, VetCore Facility (Proteomics), Vienna, Austria
[c] DSM, BIOMIN Research Center, Tulln, Austria
[d] University of Veterinary Medicine Vienna, Institute of Animal Nutrition and Functional Plant Compounds, Nutrigenomics Unit, Vienna, Austria

ARTICLE INFO

Keywords:
Cattle
Proteomics
Bovine salivary core proteome
Forage feeding
High-concentrate diets
Phytogenic feed additive

ABSTRACT

Phytogenic compounds may influence salivation or salivary properties. However, their effects on the bovine salivary proteome have not been evaluated. We investigated changes in the bovine salivary proteome due to transition from forage to high-concentrate diet, with and without supplementation with a phytogenic feed additive. Eight non-lactating cows were fed forage, then transitioned to a 65% concentrate diet (DM basis) over a week. Cows were control ($n = 4$, CON) or supplemented with a phytogenic feed additive (n = 4, PHY). Proteomic analysis was conducted using liquid chromatography coupled with mass spectrometry. We identified 1233 proteins; 878 were bovine proteins, 189 corresponded to bacteria, and 166 were plant proteins. Between forage and high-concentrate, 139 proteins were differentially abundant ($P < 0.05$), with 48 proteins having a log2FC difference $> |2|$. The salivary proteome reflected shifts in processes involving nutrient utilization, body tissue accretion, and immune response. Between PHY and CON, 195 proteins were differently abundant ($P < 0.05$), with 37 having a log2FC difference $> |2|$; 86 proteins were increased by PHY, including proteins involved in smell recognition. Many differentially abundant proteins correlated ($r > |0.70|$) with salivary bicarbonate, total mucins or pH. Results provide novel insights into the bovine salivary proteome using a non-invasive approach, and the association of specific proteins with major salivary properties influencing rumen homeostasis.

Significance: Phytogenic compounds may stimulate salivation due to their olfactory properties, but their effects on the salivary proteome have not been investigated. We investigated the effect of high-concentrate diets and supplementation with a phytogenic additive on the salivary proteome of cows. We show that analysis of cows' saliva can be a non-invasive approach to detect effects occurring not only in the gut, but also systemically including indications for gut health and immune response. Thus, results provide unique insights into the bovine salivary proteome, and will have a crucial contribution to further understand animal response in terms of nutrient utilization and immune activity due to the change from forage to a high-energy diet. Additionally, our findings reveal changes due to supplementation with a phytogenic feed additive with regard to health and olfactory stimulation. Furthermore, findings suggest an association between salivary proteins and other components like bicarbonate content.

1. Introduction

Saliva is an easily-accessible biological fluid composed by a wide range of substances, such as proteins, hormones and metabolites, which support gastrointestinal and overall animal health [1]. Therefore, research in saliva has gained much attention in recent years, and some

* Corresponding authors at: University of Veterinary Medicine Vienna, Veterinaerplatz 1, 1210 Vienna, Austria.
E-mail addresses: ezequias.castillo-lopez@vetmeduni.ac.at (E. Castillo-Lopez), susanne.kreuzer-redmer@vetmeduni.ac.at (S. Kreuzer-Redmer).
[1] These authors share first authorship.
[2] Present address: Biome Diagnostics GmbH, Vienna, Austria.

https://doi.org/10.1016/j.jprot.2022.104795
Received 19 August 2022; Received in revised form 30 November 2022; Accepted 11 December 2022
Available online 16 December 2022

studies have further suggested that the salivary proteome could allow detection of health-associated biomarkers, which could represent an alternative to analysis of blood biomarkers [2,3]. This rationale is based on the fact that the human salivary proteome contains about 30% proteins of plasma origin, which translocate into saliva via different mechanisms [2]. More specifically, plasma proteins can reach the saliva through active transportation, passive diffusion or ultrafiltration [3,4]. Therefore, it has been suggested that the salivary proteomic profile may reflect animal response in terms of metabolic and immune activity occurring not only in the salivary glands and digestive tract, but also systemically. Other studies have reported changes in salivary proteins of sheep and goats due to different feeding regimes and have suggested the potential of the ruminant salivary proteomics as a non-invasive diagnostic tool [5,6]. In this context, cows produce up to 200 L of saliva per day, which helps to buffer rumen fluid pH, supports the proliferation of the ruminal microorganisms, and aids the transport of ingesta during regurgitation [7]. Therefore, changes in salivation or physico-chemical properties of saliva are associated with major shifts in the rumen, host metabolism, and immune response [8–10].

Analysis of the salivary proteomic profile may provide insights into proteins of cattle origin as well as on proteins from rumen microbes and feed residues found in the oral cavity, which improves understanding on the interaction between the animal and its microbiota [11]. Despite substantial research showing promising results on the salivary proteome of other animal species, there is limited research on the salivary proteome of cattle, in particular, related to dietary effects [12]. Dietary supplementation of phytogenic compounds has become common in cattle feeding [13,14]. Given their olfactory properties, some of these compounds such as thyme oil and menthol may exert neural stimulation [15], which increases activity of salivary glands leading to increased salivation or variations in salivary properties [10,16]. Additionally, these compound may have anti-inflammatory properties, which is beneficial for the animals [16]. In this regard, elucidating the bovine salivary proteome and how it is affected by diet composition can provide vital information to understand the animal response in terms of nutrient metabolism, health status or immune activity.

The aims of this study were to unveil the composition of the salivary proteome of Holstein cows, and to evaluate how this proteome is affected by the change from forage to a high-concentrate ration, with and without the supplementation of a phytogenic feed additive. We also evaluated associations between differentially abundant proteins and major salivary physico-chemical properties. Our hypothesis was that animals' metabolic changes due to increased energy supply, immune response and olfactory stimulation by the feed additive would be detected in the salivary proteome.

2. Materials and methods

2.1. Animals, study design and dietary treatments

The methods and protocols followed in this experiment were approved by the institutional ethics and animal welfare committee and the national authority according to §§ 26ff. of Animal Experiments Act of Austria, Tierversuchsgesetz 2012 – TVG 2012 (protocol number: BMBWF- 68.205/0003-V/3b/2019). Additionally, the protocol complied with the ARRIVE guidelines and with the EU Directive 2010/63/EU for animal experiments.

This trial was part of a larger study evaluating the effect of feed additives on animal health, details on animal management have been previously reported [16]. Briefly, eight non-lactating, multiparous Holstein cows (890 ± 72 kg body weight; 10.8 ± 2.1 years of age) fitted with ruminal cannula (Bar Diamond, Parma, ID) were used. Cows were fed a forage diet for 1 week (45% grass silage, 45% corn silage and 10% grass hay; dry matter basis). Afterwards, cows were transitioned over a week to a high-concentrate diet (26.25% grass silage, 8.75% corn silage and 65% concentrate, dry matter basis; Supplementary Table 1). This high-concentrate diet was fed for another week. Cows were divided in two groups of 4 cows, which were balanced by body weight and by age. Then, they were allocated to a control group (CON; 889 ± 49 kg, and 11.2 ± 1.2 years old) or a group supplemented with 0.04% (DM basis) of a phytogenic feed additive (PHY, 891 ± 106 kg, and 10.3 ± 2.4 years old). The PHY was characterized by a blend of herbs, spices and their extracts or pure compounds that include menthol, thymol and eugenol (Digestarom®; BIOMIN Holding GmbH, part of DSM) [16]. Before the initiation of the study, cows consumed a forage-based diet for 5 weeks.

2.2. Collection of saliva samples

During the week of forage feeding and when the cows had been transitioned to the high-concentrate diet for a week, saliva samples were collected according to the protocol described by Castillo-Lopez et al. [17]. Briefly, cows were tied using a halter and saliva was sampled directly from the mouth, between the teeth and the cheek, using a vacuum-pump with a maximum suction power of – 80 kPa (Kataspir 30, MEDUTEK, GmbH and Co., KG., Bremen, Germany). Saliva was collected immediately before offering the morning meal. The saliva container of the pump and the hose were washed and dried between samplings. Approximately 100 mL of saliva were collected at each sampling, split in aliquots, and stored in 15 mL vials. Samples were frozen at −20 °C until further analysis. Major salivary physico-chemical properties including pH, buffer capacity, bicarbonate, phosphate, total proteins, total mucins, lysozyme activity and osmolality were evaluated following laboratory protocols detailed in Castillo-Lopez et al. [17]. Samples for proteomic analysis were stored at −80 °C.

2.3. Sample preparation for proteomic analysis

Samples were thawed and centrifuged at 15,000 ×*g* for 10 min at 4 °C (centrifuge Hermle, Z 326 K; HERMLE Labortechnik GmbH, Wehingen, Germany). To be able to analyze proteins in collected saliva samples, several preparation steps had to be performed beforehand to desalt and concentrate the proteins in samples. To remove low-molecular weight solutes, dialysis of 1 mL saliva was performed using a regenerated cellulose tubing (Visking, Roth, MWCO 14,000 Da) in 500 mL 0.1 M aqueous ammonium acetate (pH 7.0). After 1 h, the ammonium acetate was exchanged for a second dialysis step for another hour. Desalted samples were frozen at −80 °C prior to lyophilization overnight [18]. Lyophilized samples were reconstituted in 200 μL phosphate buffered saline. The protein concentration was determined using a spectrophotometer with the Pierce 660 nm reagent according to the manufacturer's protocol (DS-11 FX+, DeNovix Inc., USA). For further processing, 30 μg of the protein sample were filled up to 500 μL with 8 M Urea in 50 mM TRIS and were loaded on to a Pall 10 kDa filter. The solution was centrifuged 2 times for 20 min at 10,000 rcf. The proteins were reduced with 200 mM DTT (37 °C, 30 min) and alkylated with 500 mM IAA (37 °C, 30 min) on the filter. After washing the samples twice with 100 μL 50 mM TRIS, digestion was carried out using Trypsin/LysC Mix in a ratio of 1:25 protease:protein overnight. Digested peptides were recovered with 3 × 50 μL of 50 mM TRIS and acidified with 1 μL concentrated TFA. Before LC-MS analysis, peptide extracts were desalted and cleaned using C18 spin columns (Pierce) according to the manufacturer's protocol. The dried peptides were redissolved in 300 μL 0.1% TFA; of which, 5 μL were injected to the LC-MS/MS system.

2.4. Proteomic analysis and liquid chromatography-mass spectrometry (LC–MS/MS)

Data acquisition was performed on a LC-MS/MS system consisting of a nano-HPLC Ultimate 3000 RSLC (Thermo Scientific, Dionex) directly coupled to a high-resolution Q Exactive HF Orbitrap mass spectrometer (Thermo Scientific) using a nano-ESI ion source. Peptides were pre-concentrated on a 5-mm Acclaim PepMap μ-Precolumn (300 μm inner

diameter, 5 μm particle size, and 100 Å pore size, Thermo Scientific, Dionex) before being separated on a 25 cm Acclaim PepMap C18 column (75 μm inner diameter, 2 μm particle size, and 100 Å pore size, Thermo Scientific, Dionex). The mobile phase for sample loading was 2% ACN in ultrapure H_2O with 0.05% TFA with a flow rate of 5 μL/min, whereas for peptide separation gradient elution with a flow rate of 300 nL/min was performed. The gradient started with 4% B (80% ACN with 0.08% formic acid) for 7 min, increased to 31% in 60 min and to 44% in additional 5 min. A washing step with 95% B followed. Ultrapure H_2O with 0.1% formic acid was used as a mobile Phase A.

The MS full scans were acquired in the ranges *m/z* 350–2000 Da with a resolution of 60,000. The maximum injection time was 50 ms and the automatic gain control was set to 3eˆ6. The top 10 most intense ions were further fragmented in the Orbitrap via higher-energy collision dissociation activation over a mass range between *m/z* 200 and 2000 Da with a resolution of 15,000 and an intensity threshold of 4eˆ3. Ions with a charge state +1, +7, +8 and > +8 were excluded. Normalized collision energy was set at 28. The automatic gain control was set at 5eˆ4 and the maximum injection time was 50 ms. In order to avoid repeated peak fragmentation dynamic exclusion of precursor ion masses over a time window of 30 s was used. The database search was performed using the Proteome Discoverer Software 2.4.305 (Thermo Fisher Scientific). The protein databases were downloaded from the UniProt homepage (http://www.uniprot.org) for the following species: *Bos taurus* (taxonomy ID 9913), bacteria (taxonomy ID 2, reviewed proteins), and plant (viridiplantae, taxonomy ID 33090, reviewed proteins). Additionally to the combined UniProt databases, the common contaminant database cRAP was used (https://www.thegpm.org/crap/) with bovine proteins removed. Search settings were as follows: 10 ppm precursor mass tolerance and 0.02 Da fragment mass tolerance; dynamic modifications allowed were oxidation of methionine as well as the N-terminal protein modifications acetylation, methionine loss and the combination of both, static modification carbamidomethylation on cysteine. Only proteins with at least two identified peptides were reported. The label free quantification strategy was applied in order to compare protein abundance in the experiments. Details as well as information for analysis of each technical replicate, protein identification and number of peptides as well as the compiled raw abundance data of proteins for all cows can be found in the file deposited at https://doi.org/10.17632/5c74mnmdb3.1 [19].

2.5. Bioinformatics and statistical analysis

A statistical power analysis was conducted using a subsample of major detected proteins with Proc Power of SAS (version 9.4; SAS Institute, Cary, NC). To do so, raw abundance data were subjected to log transformation, and then the analysis was performed similar to Stroup 1999 [20], and Kononoff and Hanford 2006 [21]. Results demonstrated an acceptable statistical power, which averaged 81%, ranging from 70 to 92% with an alpha of 0.05.

The final dataset contained the raw abundances of 1273. From these, 40 proteins were absent in all technical replicates and were removed from the analysis, resulting in 1233 proteins mapped to the bovine, plant and bacterial databases. The level of concordance between technical replicates was evaluated by hierarchical cluster analysis using the "ward.D2" method (Supplementary Fig. 1). Proteins that were present in both technical replicates of each sample were considered for further analysis. After calculating the median between technical replicates, all missing values were replaced by 0 and imported into RStudio [22].

The dataset was analyzed using the DEP package v1.12.0 for differential enrichment analysis of proteomic data [23]. Only proteins present in 25% of the samples were kept, which allowed inclusion of animals from all the dietary regimes used. Normalization was performed using variance stabilizing transformation. Analysis of similarities (ANOSIM) between groups was performed using the vegan package (version 2.5.7) [24]. Differences between groups were considered significant when $P < 0.05$ and trends when $0.05 \geq P < 0.1$. Differential abundance analysis was conducted using a multivariate model (ANOVA) consisting of the effect of diet, phytogenic supplementation, and their interaction. The same model was used to evaluate numerical differences in bacterial, plant and bovine proteins between diets and treatment groups. Log2-transformed values were used to calculate the fold change (FC) between groups as a mean (forage) - mean (grain), and mean (CON) - mean (PHY).

Correlation and regression analyses were conducted with SAS using Proc corr and Proc reg, respectively, to evaluate the association between individual proteins found to be differential abundant and major salivary physico-chemical properties. Then, correlation networks were constructed using the R packages igraph v1.2.7 and ggraph v2.0.5 to illustrate the association between salivary proteins that were differentially abundant across diets and showing strongest correlations ($r \geq |0.70|$) with major salivary physico-chemical properties.

2.6. Functional enrichment

The list of the protein IDs that composed the bovine core proteome was used to determine the gene ontology (GO) terms over-represented in saliva using Protein Analysis Through Evolutionary Relationships (PANTHER) classification tool (http://www.pantherdb.org/) [25]. Protein-Protein Interaction (PPI) Networks and Functional Enrichment Analysis based on GO terms and Kyoto Encyclopedia of Genes and Genomes (KEGG) pathways was performed using the Search Tool for the Retrieval of Interacting Genes/Proteins version 11.5 (STRING, https://string-db.org/) [26].

3. Results

3.1. Protein content and distribution in saliva samples

There were 1233 proteins identified in saliva after verifying the presence in both technical replicates. From these, 878 mapped to the bovine database, while 189 were of bacterial origin and 166 of plant origin. The number of proteins per sample ranged between 888 and 1042, with an average of 959 ± 52 proteins per sample (Fig. 1). Slightly more than half of total proteins (619) were present in all samples. The 10 proteins identified with the highest numbers of identified peptides mapped to each database are listed in Table 1. No significant differences were found in the number of bovine or plant proteins between forage and high-concentrate diets ($P > 0.10$). A trend was found for a difference in the number of bacterial proteins between forage and high-concentrate feeding ($P = 0.09$), and between CON and PHY ($P = 0.05$), with CON animals having a salivary proteome enriched in bacterial proteins.

3.2. Characterization of the bovine salivary core proteome

A total of 586 bovine proteins were present in all samples (Supplementary Table 2). From these, 556 were successfully mapped using PANTHER and clustered based on their function (Supplementary Table 3). The core bovine proteome was further annotated based on GO terms according to biological process (BP), molecular function (MF) and cellular component (CC) – level 1.

Sixteen biological process terms were found to be enriched (level 2), mainly cellular process (GO:0009987, $n = 261$), metabolic process (GO:0008152, $n = 173$), biological regulation (GO:0065007, $n = 113$) and response to stimulus (GO:0050896, $n = 84$). The main subcategories found for cellular process (level 3) were cellular metabolic process (GO:0044237, $n = 149$), cellular component organization or biogenesis (GO:0071840, $n = 59$) and cellular response to stimulus (GO:0051716, $n = 49$). Many proteins were also involved in metabolic processes (level 3) associated with organic substance metabolic process (GO:0071704, $n = 158$), cellular metabolic process (GO:0044237, n = 149), primary metabolic process (GO:0044238, $n = 142$) and nitrogen compound

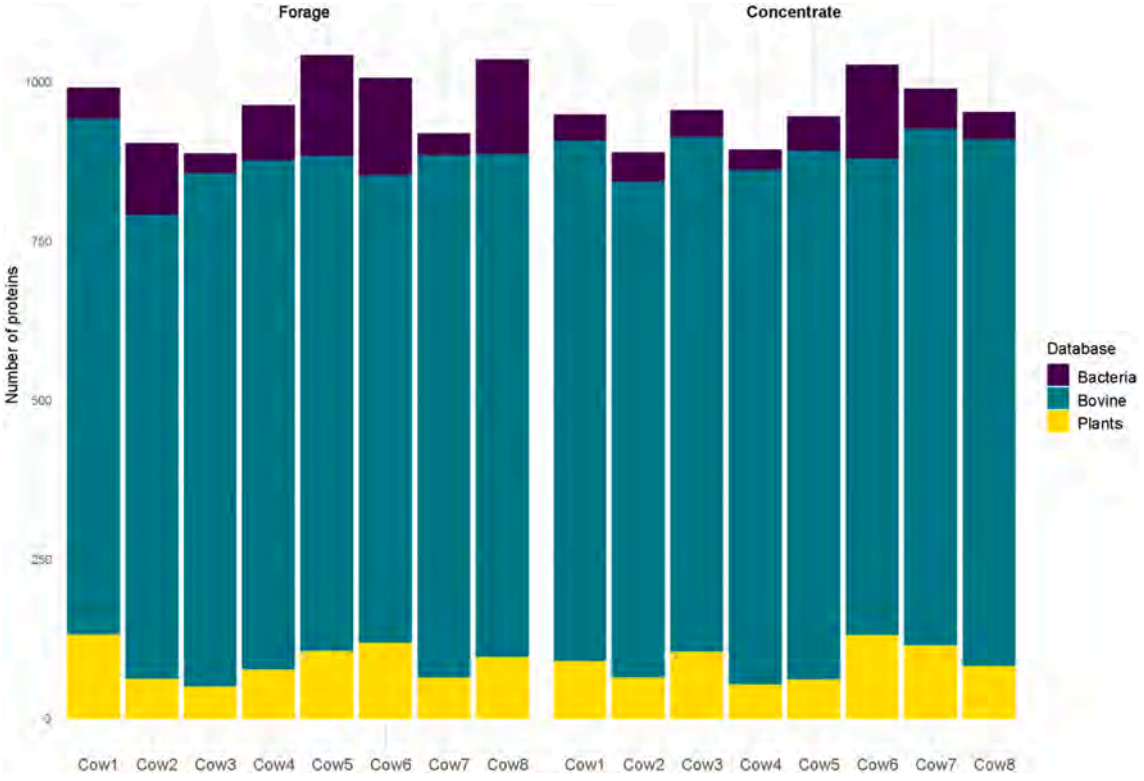

Fig. 1. Distribution of proteins from bacteria, bovine, and plants per sample when animals were fed forage or high-concentrate diet.

metabolic process (GO:0006807, $n = 137$). Concerning biological regulation, the main subcategory enriched (level 3) was regulation of biological process (GO:0050789, $n = 103$). Response to stimulus was mainly divided into level 3 subcategories associated with response to stress (GO:0006950, $n = 55$) and cellular response to stimulus (GO:0051716, n = 49).

The core proteome spanned across 8 molecular functions (level 2), such as binding (GO:0005488, $n = 202$), catalytic activity (GO:0003824, $n = 196$) and molecular function regulator (GO:0098772, $n = 50$). Binding was mainly associated with protein binding (GO:0005515, $n = 114$), ion binding (GO:0043167, $n = 56$), organic cyclic compound binding (GO:0097159, n = 50) and heterocyclic compound binding (GO:1901363, $n = 48$). The most enriched level 3 GO terms associated with catalytic activity were hydrolase activity (GO:0016787, $n = 111$) and catalytic activity, acting on a protein (GO:0140096, $n = 84$), while the most enriched molecular function regulator GO term was enzyme regulator activity (GO:0030234, $n = 44$).

Within the third analyzed GO term class, cellular components, three GO terms were enriched; namely cellular anatomical entity (GO:0110165, $n = 333$), intracellular (GO:0005622, $n = 212$) and protein-containing complex (GO:0032991, n = 48). Level 3 mostly enriched GO terms in cellular anatomical entity were cytoplasm (GO:0005737, $n = 182$), extracellular region (GO:0005576, $n = 130$), organelle (GO:0043226, $n = 127$), extracellular space (GO:0005615, $n = 126$), membrane (GO:0016020, $n = 72$), cell periphery (GO:0071944, $n = 70$) and cytosol (GO:0005829, $n = 55$). Regarding intracellular, cytoplasm (GO:0005737, n = 182) and intracellular organelle (GO:0043229, $n = 125$) were the most enriched subcategories, while in the case of protein-containing complex, catalytic complex (GO:1902494, n = 12) and membrane protein complex (GO:0098796, $n = 9$) were the most common.

3.3. Variability of protein abundance across the whole protein profile regarding diet and PHY supplementation

Principal component analysis was performed across the whole protein profile to identify sources of variability in the proteomic dataset. Principal component 1 is represented on the x-axis, with 28.49% variation and principal component 2 on the y-axis with 17.58% variation (Fig. 2). The principal component analysis plot did not show a clear separation based on diet and phytogenic supplementation. To further investigate whether there were differences between the groups, ANOSIM was performed on the Euclidean distances using diet, treatment, and animal as groups of interest. No statistically significant differences were found. However, there were some trends found regarding the phytogenic treatment ($R = 0.160$, $P = 0.07$) and diet ($R = 0.154$, $P = 0.07$). No effect was found for individual cow ($R = 0.248$, $P = 0.11$).

3.4. Differentially abundant salivary proteins for diet and feed supplementation

A total of 139 salivary proteins were differentially abundant between forage and high-concentrate diet ($P < 0.05$, Supplementary Table 4). From these, 48 proteins had a $\log_2FC > |2|$. Sixteen of these highly differentially abundant proteins mapped to the bacterial database and increased during forage feeding ($P < 0.05$). These were mainly elongation factors from different bacterial species (Q04FQ4, A9KRZ3, P42475, A6GYU7, P69952, Q3B6G3, B2UQY9, A5ELM9, Q67JU1, A6W394, A9WFP3). The bovine proteins (Table 2) that mostly increased during forage feeding were tubulin (E1BJB1, $P = 0.048$), keratinization-associated protein (F1MKE7, $P = 0.03$), tyrosine 3-monooxygenase/tryptophan 5-monooxygenase activation protein zeta (A0A4D6DKI8, $P = 0.02$) and carbonic anhydrase 2 (F1N0H3, $P = 0.01$).

Feeding high-concentrate diet increased 53 salivary proteins; from which, 13 had a $\log_2FC > |2|$. From these highly impacted proteins, the majority were plant proteins, including 5 associated with *Brassica napus* (P09893, P17333, P33525, P33522 and P24565). The bovine beta-

Table 1
Top 10 proteins with the highest numbers of identified peptides from bacteria, plants and bovine found in the saliva samples of non-lactating Holstein cows.

Accession ID	Name
Bacteria	
Q02SZ7	Lysyl endopeptidase OS=*Pseudomonas aeruginosa* (strain UCBPP-PA14)
P42475	Elongation factor Tu OS=*Fibrobacter succinogenes* (strain ATCC 19169 / S85)
Q8A463	Elongation factor Tu OS=*Bacteroides thetaiotaomicron* (strain ATCC 29148 / DSM 2079 / NCTC 10582 / E50 / VPI-5482)
A6KYK9	Elongation factor Tu OS=*Bacteroides vulgatus* (strain ATCC 8482 / DSM 1447 / JCM 5826 / NBRC 14291 / NCTC 11154)
B2RL52	Elongation factor Tu OS=*Porphyromonas gingivalis* (strain ATCC 33277 / DSM 20709 / CIP 103683 / JCM 12257 / NCTC 11834 / 2561)
B6YQ04	Elongation factor Tu OS = *Azobacteroides pseudotrichonymphae* genomovar. CFP2
C4ZBL1	Phosphoenolpyruvate carboxykinase (ATP) OS = *Agathobacter rectalis* (strain ATCC 33656 / DSM 3377 / JCM 17463 / KCTC 5835 / VPI 0990)
A4IJI7	Elongation factor Tu OS = *Geobacillus thermodenitrificans* (strain NG80–2)
A6GYU7	Elongation factor Tu OS=*Flavobacterium psychrophilum* (strain ATCC 49511 / DSM 21280 / CIP 103535 / JIP02/86)
Q7TTF9	Elongation factor Tu OS=*Haemophilus ducreyi* (strain 35000HP / ATCC 700724)
Plants	
P33525	Cruciferin CRU1 OS=*Brassica napus*
P33523	Cruciferin BnC1 OS=*Brassica napus*
Q02498	Cruciferin PGCRURSE5 OS = *Raphanus sativus*
P33522	Cruciferin CRU4 OS=*Brassica napus*
O65315	Actin OS=*Coleochaete scutata*
P04405	Glycinin G2 OS = *Glycine* max
P48688	Ribulose bisphosphate carboxylase large chain OS=*Carica papaya*
P16098	Beta-amylase OS=*Hordeum vulgare*
P93584	Actin-82 (Fragment) OS=*Solanum tuberosum*
P16347	Endogenous alpha-amylase/subtilisin inhibitor OS = *Triticum aestivum*
Bos taurus	
F2FB42	Mucin-5B
G3X6I0	Uncharacterized protein
Q2UVX4	Complement C3
F2FB39	Mucin-19 (Fragment)
Q7SIH1	Alpha-2-macroglobulin
F1MB32	Alpha-2-macroglobulin like 1
F1MB90	Uncharacterized protein
A5D7D1	Alpha-actinin-4
P02769	Serum albumin
G5E5A7	Uncharacterized protein

hexosaminidase (H7BWW2, $P < 0.001$), chondroadherin (F1MYE4, $P = 0.005$), lymphocyte-specific protein 1 (Q0P5E0, $P = 0.045$) and cathelicidin-3 (P19661, $P = 0.028$) were among those bovine proteins that most increased in the high-concentrate diet.

Between CON and PHY, 195 salivary proteins were differently abundant ($P < 0.05$, Supplementary Table 5) and 37 had a $\log_2FC > |2|$. From these, 19 were bacterial proteins, and all increased in CON. These were mainly elongation factors (A8MLC4, P42475, A6GYU7, A6KYJ7, B2UQY9, A0PXT1, P69952), enolases (Q7MTV8, Q88MF9), pyruvate-flavodoxin oxidoreductases (P03833, P52965) and phosphoenolpyruvate carboxykinases (C4Z0Q6, O83023). The CON diet led to an increase in several bovine keratins (G3N0V2, A6QNZ7, A6QNX5, Q17QL7, A4FV94, A0A3Q1MYR8, M0QVZ6) and lysozyme (A0A077S9Q3, $P = 0.002$) (Table 3). Mucins (F2FB39 and Q28908, $P < 0.03$) and odorant-binding proteins (P07435 and Q0IIA2, $P < 0.03$) were among the proteins enriched in PHY. The most up-regulated protein in PHY was interleukin-1 (F1MYY4, $P < 0.01$).

3.5. Protein-protein interaction and KEGG functional enrichment of differential abundant bovine proteins

To gain a deeper understanding on the functions of the 90 and 164 differentially abundant bovine proteins regarding diet and treatment, respectively, functional enrichment of the protein–protein interactions (PPI) networks were obtained using STRING. Eight KEGG pathways were found to be significantly enriched in the protein-protein network built based on the differentially abundant proteins between dietary regimes (Table 4). When considering the differentially abundant proteins regarding the phytogenic supplementation, twelve pathways were significantly enriched. Complement and coagulation cascades (bta04610), adherens junction (bta04520), bacterial invasion of epithelial cells (bta05100), focal adhesion (bta04510) and leukocyte transendothelial migration (bta04670) were the main pathways enriched when considering the differential abundant proteins found due to diet (Fig. 3). The first pathway was enriched due to changes in the proteins P34955 (*SERPINA1*), P41361 (*SERPINC1*), K4JDR8 (*A2M*), A6QPP2 (*SERPIND1*), Q3MHN2 (*C9*), E1BMJ0 (*SERPING1*), F1MNV5 (*KNG1*) and A0A3Q1MR54 (*C8G*), all down-regulated when the animals were fed high-concentrate. The latter 4 pathways were found to be enriched due to the common proteins P61585 (*RHOA*) and P63258 (*ACTG1*), up-regulated during high-concentrate feeding, and A0A3Q1LXR2 (*RAC1*) and A0A3Q1MN97 (*VCL*), found to be down-regulated under this condition.

The supplementation of a phytogenic feed additive led to the enrichment of pathways associated with 2-oxocarboxylic acid metabolism (bta01210), pentose phosphate pathway (bta00030), biosynthesis of amino acids (bta01230), complement and coagulation cascades (bta04610) and glycolysis/gluconeogenesis (bta00010) (Fig. 4). Mainly two clusters were observed in the PPI network: complement and coagulation cascades due to P41361 (*SERPINC1*), K4JDT2 (*A2M*), P17697 (*CLU*), P81187 (*CFB*), Q2UVX4 (*C3*), F1N0I3 (*F5*), A5D9D2 (*C4BPA*), up-regulated in PHY, and carbohydrate metabolism-associated pathways.

3.6. Salivary components and their correlation with differentially abundant proteins

Salivary physico-chemical properties were measured (Table 5) to investigate their correlation with the salivary proteome. There was a statistical interaction between diet and PHY ($P < 0.05$) for buffer capacity. More specifically, we found an increase of buffer capacity in CON due to diet change. Bicarbonate increased ($P < 0.01$), while phosphate decreased ($P < 0.05$) and mucins tended to decrease ($P = 0.06$) due to diet shift. Salivary pH, total proteins, osmolality and lysozyme activity were not affected. Strong correlations ($P < 0.01$, $r \geq |0.70|$) were found between several proteins and the salivary physico-chemical properties. Among proteins that were differentially abundant between diets, 6 were correlated with salivary pH, 51 were correlated with bicarbonate content, 33 were correlated with total mucins, and one was correlated with lysozyme activity. From these proteins, 29 were of bovine origin (Fig. 5), 25 were of bacterial origin, and 15 were of plant origin (Fig. 6A-B). In addition, from proteins that were differentially abundant between treatments, one was correlated with salivary pH, 13 were correlated with bicarbonate content, 20 were correlated with total mucins, and two were correlated with lysozyme activity. Most of the proteins that showed a positive correlation with bicarbonate content negatively correlated with mucins and vice versa. Furthermore, immune regulating proteins such as CD177 (A0A3Q1M1B6), and interleukin-1 (A4IFH0) highly correlated with bicarbonate and mucins. Another finding was the strong correlation of certain cellular cytoskeleton or energy regulating proteins, such as tubulin beta chain (E1BJB1) and the adipogenesis regulatory factor (Q2NKR5) with salivary components. From these, CD177, interleukin-1 and adipogenesis regulatory factor positively correlated with the content of total bicarbonate, but negatively correlated with

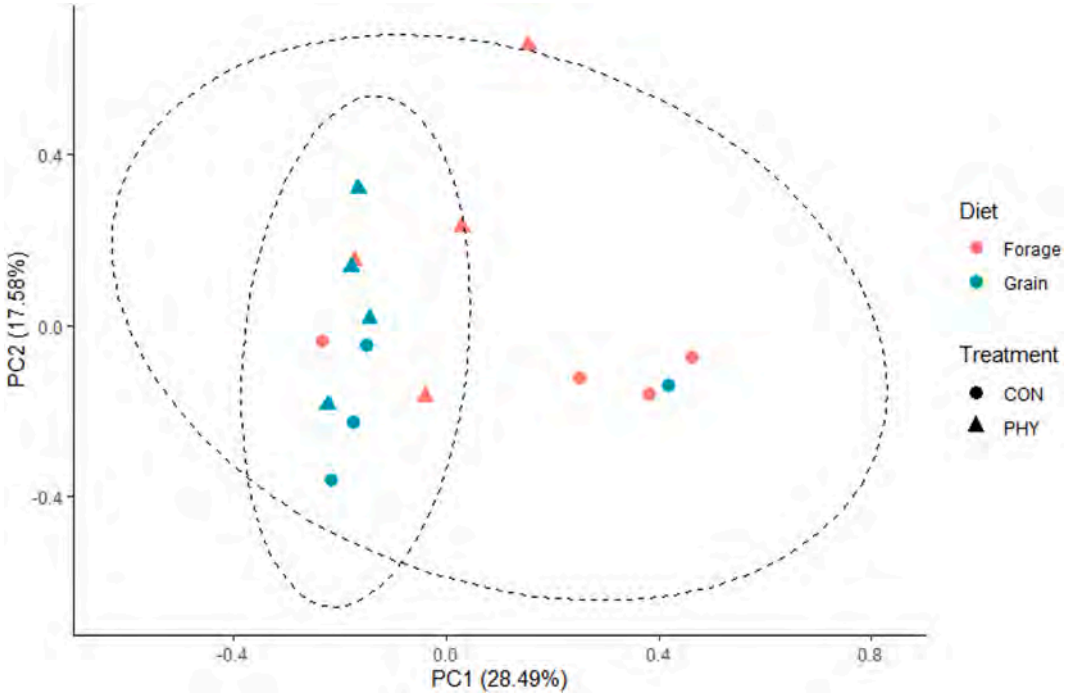

Fig. 2. Principal component analysis of the whole protein profile showing variability among samples performed on the Euclidean distances using diet and treatment as groups of interest. Trends were found regarding the phytogenic treatment ($R = 0.160$, $P = 0.07$) and diet ($R = 0.154$, $P = 0.07$).

mucins. However, tubulin beta chain positively correlated with total mucins (Fig. 7A-D).

4. Discussion

Reports from research in other animal species have suggested that the salivary proteome can be used to assess host nutrient metabolism and immune response. This rationale is based on the fact that plasma proteins can be translocated into saliva [2–4]. In this context, the main objectives of this study were to unravel the salivary proteomic profile of Holstein cows, and to evaluate how it is affected by a drastic change in diet and by the supplementation with phytogenic compounds. We detected 556 bovine proteins that compose the core proteome, which could be further classified based on their known functions. Although no clear clustering was found based on diet or supplementation, there were significant changes in the abundance of several salivary proteins that could reflect host response in terms of body tissue accretion, nutrient metabolism, or immune activity.

4.1. Core salivary proteins related to body tissue accretion and nutrient metabolism

When cattle are switched from low to high-energy diets, the additional metabolizable energy which is not used for maintenance or production contributes to body tissue accretion. It is important to note that because this study was part of a larger project, final body weight of cows was recorded after 4 weeks of high-concentrate feeding, with an overall increment of 76 kg (964 ± 49 kg of final body weight for CON and 967 ± 99 kg for PHY). Accordingly, we found important shifts in the salivary proteome that are in agreement with the cellular components and metabolic processes that were enriched and that are involved in body tissue synthesis. For example, the increased abundance of the adipogenesis regulatory factor (Q2NKR5), which plays a crucial role in adipocyte differentiation [27], may reflect increased adipose tissue accretion following increased supply of energy from the short-chain-fatty-acids such as acetic acid, the major fermentation acid used for biosynthesis of fat in ruminants. The latter observation could also reflect increased de novo fat synthesis from glucose-derived acetyl CoA [28] originating from the glucose produced from propionic acid, a major glucose precursor; biological processes occurring in mitochondria, smooth endoplasmic reticulum and cytosol. In addition to adipogenesis, our findings indicate increased molecular mechanisms involved in synthesis of body protein in cows fed high-concentrate, as revealed by increased abundance of several proteins that compose the cellular cytoskeleton, whose presence is required for appropriate tissue development [29]. This is also in agreement with the increased abundance of calreticulin (P52193) as well as chaperonin containing TCP1 subunit 5 (F1MWD3), a member of the chaperone protein family [30] present in the cytosol, which participates in different stages of protein synthesis in the ribosomes. For example, calreticulin is involved in quality control and protein folding before their transport from the rough endoplasmic reticulum to the Golgi apparatus [31], a process where chaperones are closely involved [32]. In addition, these observations support the increment in cytochrome *c* (P62894) in cows consuming the energy dense diets. Cytochrome c is one of the major complexes of the electron transport chain and plays an essential role during oxidative phosphorylation and ATP production in the mitochondrial intermembrane space [33], especially during increased nutrient supply due to high-concentrate intake.

Furthermore, our results suggest important changes in host salivary proteins associated with glucose metabolism due to diet change. Specifically, the decrease in the abundance of glyceraldehyde-3-phosphate dehydrogenase (Q2KJE5), a key glycolytic enzyme, during high-concentrate feeding may reflect regulation of glucose degradation after energy need has been met. In this regard, our findings show that synthesis of the salivary protein ras-related C3 botulinum toxin substrate 1 (A0A3Q1LXR2) decreased when cows were switched to high-concentrate diet. The latter protein has been reported to be the involved in glucose-stimulated insulin secretion [34]. Insulin promotes glycolysis by acting on the enzyme phosphofructokinase, increasing phosphorylation of fructose within the cell. Thus, the decrease of ras-related C3 botulinum toxin substrate 1 (A0A3Q1LXR2) may reflect regulation of glucose degradation to increase its storage during high-concentrate feeding.

Table 2
Bovine proteins found to be differentially abundant[1] in the saliva of non-lactating Holstein cows when fed either forage or a high-concentrate diet.

		Forage		High-concentrate			
Accession ID	Name	Mean	SD	Mean	SD	*P*-value[2]	Log_2FC[3]
E1BJB1	Tubulin beta chain	20.793	3.513	17.138	2.794	0.048	3.655
F1MKE7	IF rod domain-containing protein	22.473	2.496	19.556	2.862	0.026	2.916
A0A4D6DKI8	Tyrosine 3-monooxygenase/tryptophan 5-monooxygenase activation protein zeta (Fragment)	19.733	2.416	16.846	1.743	0.021	2.886
F1N0H3	Carbonic anhydrase 2	19.310	1.662	16.515	1.821	0.011	2.795
E1BEL8	Globin B1	21.892	1.582	19.297	2.690	0.026	2.595
Q2KJE5	Glyceraldehyde-3-phosphate dehydrogenase, testis-specific	19.389	2.619	16.870	1.254	0.024	2.519
F1MIU2	BCL2 associated athanogene 3	21.238	1.980	18.815	2.578	0.031	2.423
A0A140T8C5	Uteroglobin	24.001	0.959	22.101	1.678	0.02	1.899
E1BBX7	Lipocln_cytosolic_FA-bd_dom domain-containing protein	24.449	1.695	22.861	1.719	0.021	1.588
A0A3Q1LXR2	Ras-related C3 botulinum toxin substrate 1	18.652	1.277	17.103	1.469	0.01	1.549
F1MTK7	Protein FAM107B	21.654	1.235	20.132	1.107	0.032	1.523
A0A3Q1M193	Glycoprotein 2	20.619	2.081	19.122	2.868	0.033	1.497
G1K122	Retinol-binding protein	20.211	0.866	18.854	0.434	0.002	1.358
A0A3Q1MR54	Lipocln_cytosolic_FA-bd_dom domain-containing protein	19.964	0.617	18.680	1.271	0.033	1.284
A6QNW7	CD5 molecule like	21.801	0.811	20.576	1.299	0.046	1.226
E1BMJ0	Serpin family G member 1	21.267	0.906	20.069	1.153	0.035	1.198
Q2T9X2	T-complex protein 1 subunit delta	23.494	0.645	22.316	0.387	0.001	1.178
A0A3Q1MB09	Aminopeptidase	22.882	0.915	21.733	0.797	0.023	1.149
P34955	Alpha-1-antiproteinase	25.185	0.370	24.058	0.819	0.003	1.127
P41361	Antithrombin-III	22.885	0.528	21.786	0.842	0.003	1.099
G3N1U4	Serpin A3–3	22.127	0.560	21.098	1.028	0.019	1.029
E1BKM4	Programmed cell death 6 interacting protein	22.745	0.743	21.731	0.397	0.007	1.014
G3MX54	Dynein light chain	20.577	0.389	19.619	0.852	0.01	0.958
Q3T0K2	T-complex protein 1 subunit gamma	20.163	0.861	19.268	0.337	0.018	0.896
A0A3Q1M3Z5	Cathepsin D	24.338	0.381	23.443	0.633	0.002	0.895
K4JDR8	Alpha-2-macroglobulin variant 5	23.316	0.846	22.427	0.767	0.05	0.889
P01045	Kininogen-2	21.186	0.603	20.314	0.871	0.046	0.872
A0A0A0MP92	Serpin A3–7	22.750	0.899	21.891	1.053	0.048	0.859
Q3MHN2	Complement component C9	21.420	0.632	20.563	0.460	0.01	0.856
B0JYQ0	ALB protein	22.347	0.585	21.491	0.848	0.041	0.856
Q3ZBZ1	45 kDa calcium-binding protein	23.776	0.618	22.942	0.577	0.024	0.834
F1MNV5	Kininogen-1	21.493	0.682	20.661	0.799	0.049	0.832
P02769	Serum albumin	29.439	0.695	28.638	0.698	0.032	0.802
A6QPP2	SERPIND1 protein	21.349	0.623	20.553	0.464	0.016	0.796
A0A3Q1M2G6	Lipocln_cytosolic_FA-bd_dom domain-containing protein	31.678	0.658	30.898	0.701	0.032	0.780
Q9TTE1	Serpin A3–1	23.388	0.527	22.629	0.698	0.03	0.759
Q58CQ9	Pantetheinase	24.527	0.698	23.834	0.642	0.049	0.692
G3X8E3	Beta-microseminoprotein	28.906	0.672	28.255	0.281	0.035	0.651
F1MMK9	Protein AMBP	23.210	0.516	22.584	0.503	0.018	0.626
Q27971	Calpain-2 catalytic subunit	20.160	0.630	19.545	0.600	0.047	0.614
F1N647	Fatty acid synthase	17.059	0.700	16.446	0.525	0.048	0.613
A1A4N6	Sulfotransferase	18.583	0.585	17.979	0.301	0.016	0.603
G3X6N3	Serotransferrin	24.299	0.603	23.707	0.427	0.03	0.592
Q2KJH4	WD repeat-containing protein 1	24.490	0.477	23.901	0.280	0.012	0.589
Q6EWQ7	Eukaryotic translation initiation factor 5A-1	23.326	0.578	22.805	0.416	0.028	0.521
A0A3Q1M924	Uncharacterized protein	24.057	0.305	23.781	0.474	0.015	0.276
A0A3Q1MN97	Vinculin	24.738	0.359	24.479	0.239	0.048	0.258
A0A3Q1N9B4	Ubiquitin-conjugating enzyme E2 N	23.452	0.163	23.725	0.298	0.038	−0.273
G3N2V5	HATPase_c domain-containing protein	20.325	0.404	20.670	0.263	0.046	−0.345
P63258	Actin, cytoplasmic 2	23.668	0.304	24.078	0.406	0.046	−0.410
P52193	Calreticulin	23.212	0.352	23.650	0.308	0.018	−0.438
Q32LA7	Histone H2A.V	19.040	0.354	19.488	0.424	0.049	−0.448
A0A3Q1LMK6	Uncharacterized protein	23.265	0.654	23.744	0.581	0.047	−0.479
F1MWD3	Chaperonin containing TCP1 subunit 5	19.213	0.353	19.708	0.442	0.018	−0.495
Q5E9F5	Transgelin-2	24.871	0.333	25.367	0.421	0.019	−0.496
E1BAU5	Uncharacterized protein	21.793	0.424	22.293	0.485	0.037	−0.500
P61585	Transforming protein RhoA	21.073	0.453	21.596	0.329	0.03	−0.523
P31081	60 kDa heat shock protein, mitochondrial	20.863	0.549	21.398	0.296	0.022	−0.536
M5FK93	Marapsin-like	23.164	0.301	23.701	0.487	0.025	−0.537
A6QLZ0	Galectin	23.401	0.432	23.983	0.394	0.015	−0.582
F1MM32	Sulfhydryl oxidase	26.113	0.509	26.700	0.410	0.027	−0.587
P62894	Cytochrome c	23.443	0.540	24.040	0.419	0.026	−0.598
A0A3Q1M1M7	Junction plakoglobin	21.020	0.687	21.714	0.416	0.021	−0.694
P04272	Annexin A2	25.523	0.437	26.227	0.487	0.011	−0.704
F1N6D1	WAP domain-containing protein	25.789	0.417	26.514	0.392	0.005	−0.725
A4IFH0	Interleukin-1	22.710	0.380	23.461	0.666	0.015	−0.751
Q2KJ93	Cell division control protein 42 homolog 1	20.431	0.524	21.199	0.547	0.012	−0.768
G3MXK8	Proteinase 3	22.780	0.908	23.594	0.281	0.036	−0.815
Q3MHP1	Ubiquitin-conjugating enzyme E2 L3	19.159	0.781	20.011	0.656	0.047	−0.853
P25417	Cystatin-B	22.192	0.367	23.109	0.619	0.003	−0.917
P10152	Angiogenin-1	21.600	1.077	22.556	0.871	0.032	−0.956
Q3SZ18	Hypoxanthine-guanine phosphoribosyltransferase	21.139	0.496	22.111	0.849	0.012	−0.972
A0A3Q1LUD9	Uncharacterized protein	16.881	0.752	17.878	0.545	0.015	−0.997

(*continued on next page*)

Table 2 (*continued*)

Accession ID	Name	Forage		High-concentrate			
		Mean	SD	Mean	SD	*P*-value[2]	Log_2FC[3]
P61287	Serine/threonine-protein phosphatase PP1-gamma catalytic subunit	19.342	0.893	20.437	0.764	0.024	−1.095
Q58DP6	Ribonuclease A family member 4	21.088	1.026	22.186	0.708	0.023	−1.098
P31098	Osteopontin-K	20.255	1.223	21.368	0.998	0.022	−1.114
F2Z4F5	Dipeptidyl peptidase 3	16.650	0.758	17.820	0.779	0.012	−1.169
A0A3Q1MHX8	RAB2A, member RAS oncogene family	16.413	0.641	17.651	1.741	0.018	−1.238
A0A3Q1M1B6	CD177 molecule	22.586	1.412	23.879	0.403	0.039	−1.293
Q0V7N1	Sushi domain containing 2 (Fragment)	19.125	0.950	20.428	1.223	0.035	−1.303
Q8HXK9	Apoptosis-associated speck-like protein containing a CARD	17.781	1.191	19.150	0.991	0.038	−1.368
Q2NKR5	Adipogenesis regulatory factor	22.166	1.216	23.595	0.546	0.005	−1.429
A0A3Q1LHR9	Tripeptidyl-peptidase 1	21.024	1.547	22.476	1.033	0.011	−1.452
B5B3R8	Alpha S1 casein	16.489	0.700	18.183	1.548	0.012	−1.693
E1BBP5	V-set and immunoglobulin domain containing 8	17.176	1.470	18.961	0.987	0.017	−1.784
A0A3Q1LSS3	Vasodilator-stimulated phosphoprotein	17.116	1.708	19.083	0.630	0.012	−1.967
P19661	Cathelicidin-3	20.808	1.939	22.875	1.059	0.028	−2.068
Q0P5E0	Lymphocyte-specific protein 1	19.042	2.413	21.114	0.612	0.045	−2.072
F1MYE4	Chondroadherin	16.852	0.913	18.981	1.388	0.005	−2.129
H7BWW2	Beta-hexosaminidase	17.101	1.746	20.046	0.591	0.001	−2.945

[1] Protein abundance values were normalized and log2 transformed.
[2] Significant differences were considered when $P < 0.05$.
[3] Log2-transformed values were used to calculate the fold change (FC) between groups as a mean (forage) - mean (high-concentrate).

Referring to salivary proteome changes caused by PHY, we observed that salivary zinc-alpha-2-glycoprotein (A0A452DK44), codified by *AZGP1* gene, increased in PHY. In agreement with the latter findings, this gene was up-regulated in the ruminal epithelium by the same PHY supplement [35]. This gene has been associated with lipid mobilization and glucose utilization [36], processes occurring in mitochondria and cytoplasm. Thus, although we did not measure changes in body fat or blood glucose in this study, our findings may reflect a stimulatory effect of PHY in the utilization of these nutrients.

4.2. Core salivary proteins related to ruminal and liver structural changes

High-concentrate feeding has been linked to major structural changes in the ruminal and hepatic tissues, such as ruminal papillae damage and scarring as well as liver abscess in cattle [8,37]. It is possible that such effects were reflected in the enrichment of several KEGG pathways such as cellular development and proliferation, anatomical structure morphogenesis, tissue remodeling and coagulation cascade. For example, we observed a greater abundance of angiogenin (P10152) in cows consuming the high-concentrate diet and particularly in CON compared to PHY. Angiogenin plays an essential role in the development of new blood vessels during angiogenesis [38]. Thus, our findings may reflect the host reaction involving tissue growth or repair following damage of the ruminal papilla or liver tissues, commonly observed in cattle fed high-concentrate rations. Accordingly, the greater angiogenin (P10152) in the saliva of PHY cows may reflect enhanced new blood vessel formation or tissue repair in the ruminal epithelium or liver, which is supported by the increased production of ruminal butyrate with PHY [39], a metabolite that promotes ruminal papillae growth. We also found decreased content of antithrombin-III (P41361) in the saliva of cows fed high-concentrate. Anti-thrombin inhibits enzymes associated with blood clotting in the coagulation cascade [40]. Therefore, the lower content of antithrombin during high starch feeding possibly reflects a response to allow normal activity of coagulation enzymes to enhance tissue repair and healing. However, the higher abundance of this enzyme in PHY cows suggests greater inhibition of enzymes participating in the coagulation process. Despite this observation, cows supplemented with PHY had increased content of salivary tropomyosin (F6QQ60), a main component of cellular cytoskeleton, which is involved in wound healing providing cellular support [41,42]. Therefore, the increase abundance of antithrombin in PHY-supplemented cows seems to be compensated by mechanisms resulting in enhanced cellular cytoskeleton conformation. This finding may reflect an attempt from the animals to stimulate tissue repair resulting in enhancement of processes that yield precursors for nucleotide synthesis, such as enrichment of the pentose phosphate pathway, as our results show.

Another process influenced by diet composition is the keratinization of the ruminal epithelium. Supporting our observations indicating greater keratinization-associated protein with forage (F1MKE7), keratinization has been shown to be greater when feeding a high fiber diet, likely due to increased friction of the roughage with the ruminal papillae [43]. Ruminal acidosis can also cause hardening of the ruminal epithelium, which leads to cell death and parakeratosis [37], a condition that could impair absorption of nutrients [44]. However, it is worth noting that keratins have been found to be common contaminants during proteomic sample processing [45].

4.3. Core salivary proteins related to immune response

In cattle fed high-concentrate diets, damage of the ruminal epithelium allows bacteria to gain access into circulation [46]. Additionally, a drastic change in ration composition has been suggested to increase the risk for proliferation of pathogens in the gut because of the creation of niches that allow establishment and growth of potentially pathogenic bacteria. Thus, several host proteins found in saliva may indicate a response linked to some of the KEGG pathways enriched such as bacterial invasion, immune response, leucocyte activation and cytokine production. For example, we observed an up-regulation of lymphocyte-specific protein 1 (Q0P5E0) and interleukin-1 (A4IFH0) due to high-concentrate feeding. Interleukin-1 is a cytokine that has been detected following bacterial infection [47,48]. In addition, CD177 (A0A3Q1M1B6), a surface glycoprotein involved in neutrophil proliferation and activation [49] and a crucial player in innate immune response, was up-regulated when cows were fed the high-concentrate diet. Thus, it is possible that the increase in these proteins reflected the host immune response due to translocation of bacteria from the rumen to the blood and liver. The greater abundance of interleukin-1 (F1MYY4) in PHY cows probably indicates a stronger immune response. This is an interesting finding because phytogenic supplements are suggested to have an anti-inflammatory effects in dairy cows, resulting in a reduced acute phase response during a high concentrate feeding challenge [16]. In this regard, the high abundance of the polymeric immunoglobulin receptor (P81265) in saliva samples may reflect host immune response, given the role of this protein in the transport of immunoglobulins across the epithelial cells [50]. In particular, glycoprotein 2 (A0A3Q1M193) has been shown to serve as an uptake receptor

Table 3
Bovine proteins found to be differentially abundant[1] in the saliva of non-lactating Holstein cows when fed a control diet (CON) or a ration supplemented with a phytogenic feed additive (PHY).

		CON		PHY			
Accession ID	Name	Mean	SD	Mean	SD	*P*-value[2]	Log_2FC[3]
A0A3Q1M193	Glycoprotein 2	21.904	1.505	17.837	1.505	<0.001	4.067
G3N0V2	Keratin 1	19.996	1.683	16.701	1.683	0.001	3.295
A6QNZ7	Keratin 10 (Epidermolytic hyperkeratosis; keratosis palmaris et plantaris)	20.548	1.915	17.316	1.915	0.009	3.231
F1MKE7	IF rod domain-containing protein	22.398	2.139	19.631	2.139	0.032	2.767
A6QNX5	Keratin, type II cytoskeletal 78	21.056	1.172	18.548	1.172	0.011	2.508
Q17QL7	KRT15 protein	20.601	1.279	18.175	1.279	0.008	2.425
F1MIU2	BCL2 associated athanogene 3	21.218	1.840	18.835	1.840	0.033	2.384
P60661	Myosin light polypeptide 6	18.997	0.854	16.642	0.854	0.014	2.355
P61223	Ras-related protein Rap-1b	21.397	0.266	19.054	0.266	0.023	2.343
P54229	Cathelicidin-5	23.658	0.473	21.764	0.473	0.008	1.895
A5D9D1	Vanin 2	20.045	0.503	18.182	0.503	0.015	1.863
A0A077S9Q3	Lysozyme	20.712	0.928	18.861	0.928	0.002	1.85
A7MBI6	GLOD4 protein	19.054	1.399	17.207	1.399	0.016	1.846
Q1RMM9	Alpha-galactosidase	19.309	1.379	17.484	1.379	0.034	1.824
A0A3Q1LXR2	Ras-related C3 botulinum toxin substrate 1	18.773	0.863	16.982	0.863	0.004	1.791
A0A3Q1LP81	Dihydropyrimidine dehydrogenase [NADP(+)]	21.980	0.487	20.301	0.487	0.012	1.679
F1MU22	Carboxylic ester hydrolase	20.187	1.348	18.525	1.348	0.018	1.662
A0A3Q1LI53	Nectin cell adhesion molecule 1	19.273	0.912	17.636	0.912	0.008	1.638
Q32KN6	Phosphoglycerate kinase	20.293	1.035	18.732	1.035	0.036	1.561
A0A3Q1LTY4	WAP domain-containing protein	22.247	0.515	20.724	0.515	0.029	1.524
P12344	Aspartate aminotransferase, mitochondrial	23.113	0.991	21.597	0.991	0.021	1.515
F2Z4K0	Tubulin alpha chain	18.142	1.782	16.649	1.782	0.043	1.493
P07107	Acyl-CoA-binding protein	25.519	0.470	24.172	0.470	0.001	1.348
Q17QQ2	Thiopurine *S*-methyltransferase	21.219	0.457	19.892	0.457	0.001	1.328
A0A3Q1LJB2	IF rod domain-containing protein	25.061	0.830	23.737	0.830	0.009	1.323
A0A3Q1MR14	Galectin	20.661	0.839	19.426	0.839	0.012	1.236
P81125	Alpha-soluble NSF attachment protein	19.397	0.514	18.171	0.514	0.015	1.226
P08166	Adenylate kinase 2, mitochondrial	20.480	1.331	19.266	1.331	0.025	1.213
E1BIP8	Serpin family B member 13	17.372	0.657	16.201	0.657	0.021	1.17
Q29RN2	Glycogenin 1	23.026	0.855	21.881	0.855	0.011	1.145
Q32PD5	40S ribosomal protein S19	18.987	0.653	17.920	0.653	0.008	1.067
A0A3Q1MHX8	RAB2A, member RAS oncogene family	17.556	1.581	16.509	1.581	0.039	1.047
E1BL62	Aldehyde oxidase 4	24.263	1.035	23.232	1.035	0.034	1.032
A0A3Q1NJX5	Osteoclast-stimulating factor 1	23.933	0.789	22.941	0.789	0.022	0.992
A4FV94	KRT6A protein	24.373	0.588	23.418	0.588	0.003	0.956
A0A140T8A5	Isocitrate dehydrogenase [NADP]	25.349	0.568	24.425	0.568	0.003	0.924
Q6TNF3	Transglutaminase 1	21.744	0.333	20.839	0.333	0.027	0.905
A0A3Q1MYR8	Keratin 3	23.845	0.827	22.952	0.827	0.041	0.893
A0A3Q1MH36	Protein FAM49B	21.189	0.489	20.321	0.489	0.031	0.868
A0A452DJ78	Ubiquitin-conjugating enzyme E2 variant 1	21.086	0.273	20.300	0.273	0.003	0.786
Q29RK1	Citrate synthase, mitochondrial	21.432	0.451	20.647	0.451	0.017	0.785
Q24K02	Insulin-degrading enzyme	22.010	0.454	21.246	0.454	0.013	0.764
A0A3Q1LGW7	IF rod domain-containing protein	23.519	0.455	22.809	0.455	0.007	0.71
A0A3Q1M924	Uncharacterized protein	24.239	0.123	23.599	0.123	0.001	0.639
Q5E956	Triosephosphate isomerase	27.162	0.512	26.525	0.512	0.005	0.637
Q3T0X5	Proteasome subunit alpha type-1	21.288	0.569	20.660	0.569	0.036	0.629
Q3MHR7	Actin-related protein 2/3 complex subunit 2	24.185	0.376	23.565	0.376	0.002	0.62
A0A3Q1MM92	Xanthine dehydrogenase/oxidase	21.756	0.426	21.156	0.426	0.033	0.599
A0A3Q1M3K7	Ras-related protein Rab-7a	20.771	0.331	20.177	0.331	0.009	0.594
F1N3A1	Thrombospondin-1	25.247	0.375	24.664	0.375	0.005	0.583
F1MCK2	AHNAK nucleoprotein	23.616	0.448	23.036	0.448	0.008	0.58
Q6EWQ7	Eukaryotic translation initiation factor 5A-1	23.354	0.608	22.776	0.608	0.017	0.578
M0QVZ6	Keratin, type II cytoskeletal 5	22.818	0.494	22.242	0.494	0.027	0.576
Q3MHL4	Adenosylhomocysteinase	25.553	0.434	24.996	0.434	0.012	0.557
A6H7J6	Protein disulfide-isomerase	27.239	0.263	26.702	0.263	0.001	0.538
P55052	Fatty acid-binding protein 5	29.074	0.233	28.541	0.233	0.001	0.533
F6Q816	Aminotran_1_2 domain-containing protein	23.464	0.382	22.941	0.382	0.045	0.523
Q148C3	Lymphocyte antigen 6D	24.087	0.283	23.569	0.283	0.011	0.518
Q0VCM4	Glycogen phosphorylase, liver form	24.840	0.153	24.327	0.153	0.001	0.513
Q3T0Q4	Nucleoside diphosphate kinase B	24.767	0.268	24.262	0.268	0.004	0.505
P62261	14–3-3 protein epsilon	25.482	0.367	24.981	0.367	0.019	0.501
P19858	L-lactate dehydrogenase A chain	24.173	0.476	23.687	0.476	0.036	0.486
P68252	14–3-3 protein gamma	24.199	0.304	23.748	0.304	0.015	0.451
P10462	Protein S100-A2	27.447	0.399	26.998	0.399	0.016	0.45
A0A452DJC8	Poly(U)-specific endoribonuclease	27.069	0.310	26.620	0.310	0.015	0.449
Q3ZCJ2	Aldo-keto reductase family 1 member A1	24.582	0.260	24.160	0.260	0.004	0.422
Q5E9I6	ADP-ribosylation factor 3	22.222	0.283	21.822	0.283	0.026	0.4
A0A3S5ZPM3	6-phosphogluconate dehydrogenase, decarboxylating	25.092	0.284	24.695	0.284	0.014	0.397
A0A3Q1MN97	Vinculin	24.804	0.335	24.413	0.335	0.006	0.391
F1MB32	Alpha-2-macroglobulin like 1	29.683	0.390	29.294	0.390	0.039	0.389
Q0VC36	14–3-3 protein sigma	29.553	0.370	29.183	0.370	0.037	0.371
A0A3S5ZPB5	Extracellular matrix protein 1	24.635	0.309	24.271	0.309	0.031	0.364

(*continued on next page*)

Table 3 (*continued*)

		CON		PHY			
Accession ID	Name	Mean	SD	Mean	SD	*P*-value[2]	Log_2FC[3]
A7MB62	Actin-related protein 2	23.306	0.295	22.953	0.295	0.023	0.353
Q3T0P6	Phosphoglycerate kinase 1	24.621	0.356	24.276	0.356	0.046	0.345
A7YY28	Protein ABHD14B	23.349	0.265	23.015	0.265	0.021	0.333
Q0VCX2	Endoplasmic reticulum chaperone BiP	25.784	0.258	25.471	0.258	0.03	0.313
P63103	14–3-3 protein zeta/delta	26.828	0.298	26.529	0.298	0.045	0.299
G5E5C8	Transaldolase	23.431	0.186	23.137	0.186	0.013	0.294
F1MB08	Alpha-enolase	28.165	0.191	27.873	0.191	0.023	0.292
F1MMK2	Glucose-6-phosphate 1-dehydrogenase	25.857	0.143	25.612	0.143	0.006	0.245
Q3ZCL0	Cysteine-rich secretory protein 2	27.630	0.217	28.096	0.217	0.027	−0.465
G3X6I0	Uncharacterized protein	30.102	0.454	30.610	0.454	0.048	−0.508
E1BLA8	Golgi membrane protein 1	24.179	0.440	24.704	0.440	0.049	−0.525
P81187	Complement factor B	24.118	0.455	24.654	0.455	0.034	−0.535
F1MWI1	Clusterin	22.496	0.432	23.040	0.432	0.035	−0.543
Q2KIS7	Tetranectin	22.175	0.272	22.762	0.272	0.004	−0.586
E1BDN9	Family with sequence similarity 3 member D	21.518	0.388	22.115	0.388	0.012	−0.596
Q2UVX4	Complement C3	29.018	0.371	29.624	0.371	0.011	−0.606
P17697	Clusterin	24.911	0.478	25.595	0.478	0.014	−0.684
P41361	Antithrombin-III	21.991	1.053	22.680	1.053	0.038	−0.688
A0A452DHZ5	Nucleobindin-1	24.856	0.266	25.549	0.266	0.009	−0.693
Q0IIH5	Nucleobindin-2	25.585	0.357	26.330	0.357	0.014	−0.746
P01888	Beta-2-microglobulin	24.997	0.310	25.759	0.310	0.021	−0.762
F2FB39	Mucin-19 (Fragment)	29.855	0.442	30.641	0.442	0.009	−0.785
Q0VCK0	Bifunctional purine biosynthesis protein PURH	18.207	0.888	19.000	0.888	0.05	−0.793
Q5EA41	Polypeptide *N*-acetylgalactosaminyltransferase 6	22.290	0.906	23.083	0.906	0.045	−0.794
A0A452DK44	Zinc-alpha-2-glycoprotein	26.641	0.353	27.438	0.353	0.027	−0.797
A0A3Q1MFL7	Destrin	20.386	0.323	21.183	0.323	0.001	−0.798
F6QQ60	Tropomyosin 4	18.815	0.545	19.636	0.545	0.005	−0.82
A7MBH9	G protein subunit alpha i2	22.365	0.307	23.195	0.307	0.002	−0.83
G3X700	Lipocln_cytosolic_FA-bd_dom domain-containing protein	31.712	0.402	32.550	0.402	0.003	−0.838
A0A3Q1LMK6	Uncharacterized protein	23.079	0.568	23.930	0.568	0.002	−0.851
B3VTM3	Lactoferrin	25.529	0.270	26.388	0.270	0.007	−0.86
Q28908	Mucin (Fragment)	23.463	0.628	24.325	0.628	0.024	−0.862
P00829	ATP synthase subunit beta, mitochondrial	26.162	0.721	27.108	0.721	0.017	−0.946
A0A3Q1N0C4	Uncharacterized protein	26.193	0.506	27.162	0.506	0.004	−0.969
A1A4R1	Histone H2A type 2-C	22.173	1.093	23.156	1.093	0.023	−0.983
A6QLX6	Polypeptide *N*-acetylgalactosaminyltransferase	18.698	0.907	19.682	0.907	0.019	−0.983
F1MB90	Uncharacterized protein	28.725	0.678	29.740	0.678	0.022	−1.015
Q3SX32	Perilipin	17.983	1.041	19.004	1.041	0.042	−1.021
P60986	Prolactin-inducible protein homolog	27.667	0.573	28.693	0.573	0.033	−1.026
K4JDT2	Alpha-2-macroglobulin variant 20	21.361	0.934	22.393	0.934	0.029	−1.033
A0A3Q1LIS3	SPARC like 1	21.700	1.090	22.752	1.090	0.019	−1.052
A6QPK0	SCGB2A2 protein	27.754	0.457	28.836	0.457	0.016	−1.082
A0A452DI43	Peroxiredoxin-4	20.571	0.329	21.660	0.329	0.001	−1.089
P61823	Ribonuclease pancreatic	25.833	0.823	26.950	0.823	0.028	−1.118
Q7SIH1	Alpha-2-macroglobulin	25.048	0.964	26.180	0.964	0.008	−1.132
F1N0I3	Coagulation factor V	23.138	0.602	24.282	0.602	0.028	−1.144
A5D9D2	Complement component 4 binding protein, alpha chain	20.207	0.927	21.356	0.927	0.024	−1.148
F1MHS5	Protein S100-A9	24.486	1.211	25.697	1.211	0.034	−1.212
Q0IIA2	Odorant-binding protein-like	28.549	0.583	29.761	0.583	0.012	−1.212
P20811	Calpastatin	22.306	0.477	23.519	0.477	0.049	−1.213
A0A0A0MP92	Serpin A3–7	21.712	1.048	22.928	1.048	0.009	−1.216
P10152	Angiogenin-1	21.468	0.799	22.688	0.799	0.009	−1.22
E1BJP1	Lipocln_cytosolic_FA-bd_dom domain-containing protein	27.851	0.734	29.079	0.734	0.006	−1.229
Q5DPW9	Cystatin E/M	22.517	0.700	23.760	0.700	0.002	−1.243
F1N152	Serine protease HTRA1	19.253	1.117	20.495	1.117	0.043	−1.243
Q32KV6	Nucleotide exchange factor SIL1	18.332	0.679	19.652	0.679	0.007	−1.32
F1N6V7	ST6 *N*-acetylgalactosaminide alpha-2,6-sialyltransferase 1	18.487	0.671	19.817	0.671	0.002	−1.33
P55906	Transforming growth factor-beta-induced protein ig-h3	17.901	1.232	19.232	1.232	0.023	−1.331
G3MZU3	Lipocln_cytosolic_FA-bd_dom domain-containing protein	27.141	0.497	28.479	0.497	0.001	−1.338
Q1RMN8	Immunoglobulin light chain, lambda gene cluster	24.878	1.176	26.239	1.176	0.014	−1.361
F1MW03	Thiosulfate sulfurtransferase like domain containing 1	18.635	0.927	19.996	0.927	0.002	−1.361
A0A0A0MPA0	SERPIN domain-containing protein	22.246	1.578	23.610	1.578	0.036	−1.364
A0A3Q1LSR5	Lipocln_cytosolic_FA-bd_dom domain-containing protein	24.058	0.658	25.441	0.658	0.001	−1.384
G3X701	Lipocln_cytosolic_FA-bd_dom domain-containing protein	22.329	1.171	23.741	1.171	0.049	−1.412
Q28910	Mucin (Fragment)	26.053	0.729	27.467	0.729	0.004	−1.413
P23805	Conglutinin	17.008	1.182	18.440	1.182	0.014	−1.432
A6QQF6	Suprabasin	26.026	1.791	27.471	1.791	0.034	−1.445
P31098	Osteopontin-K	20.081	1.216	21.542	1.216	0.005	−1.462
A6H6Y6	NPDC1 protein	17.799	1.540	19.281	1.540	0.048	−1.482
A0A3Q1M762	Uncharacterized protein	19.820	1.668	21.308	1.668	0.031	−1.487
A0A3Q1M1V3	Uncharacterized protein	25.890	0.727	27.391	0.727	0.001	−1.501
Q95122	Monocyte differentiation antigen CD14	19.175	1.181	20.693	1.181	0.022	−1.518
H7BWW2	Beta-hexosaminidase	17.792	2.078	19.355	2.078	0.008	−1.563
G3N0S9	Uncharacterized protein	18.981	1.862	20.550	1.862	0.05	−1.569

(*continued on next page*)

Table 3 (*continued*)

Accession ID	Name	CON Mean	CON SD	PHY Mean	PHY SD	*P*-value[2]	Log_2FC[3]
G3MZ19	Jacalin-type lectin domain-containing protein	29.125	0.562	30.713	0.562	0.01	−1.587
P02081	Hemoglobin fetal subunit beta	17.013	1.172	18.620	1.172	0.027	−1.607
A0A3Q1NE33	BPI fold-containing family A member 1	23.727	1.164	25.339	1.164	0.028	−1.612
A0A3Q1MDA4	Dystroglycan	19.902	1.189	21.540	1.189	0.007	−1.638
A0A3Q1LWV8	Ig-like domain-containing protein	25.133	1.553	26.798	1.553	0.044	−1.665
P56658	Adenosine deaminase	16.309	1.176	17.979	1.176	0.037	−1.67
A0A3Q1LHR9	Tripeptidyl-peptidase 1	20.913	1.593	22.587	1.593	0.005	−1.674
A0A452DJD0	Secretoglobin family 1D member	27.997	0.604	29.778	0.604	0.001	−1.781
Q28194	Thrombospondin-1 (Fragment)	18.179	1.182	20.024	1.182	0.008	−1.845
A0A3Q1LK49	Inter-alpha-trypsin inhibitor heavy chain H2	19.260	1.999	21.154	1.999	0.039	−1.894
F1MHX2	BPI1 domain-containing protein	23.614	1.355	25.538	1.355	0.017	−1.924
A1A4Q6	Peptidase inhibitor 3, skin-derived (SKALP)	19.220	1.671	21.167	1.671	0.047	−1.946
Q05927	5′-nucleotidase	24.001	1.140	25.960	1.140	0.028	−1.96
F1N2J8	Chromosome 25 C16orf89 homolog	16.470	1.294	18.519	1.294	0.004	−2.049
P01966	Hemoglobin subunit alpha	27.228	1.904	29.555	1.904	0.039	−2.327
E1BBX7	Lipocln_cytosolic_FA-bd_dom domain-containing protein	22.470	0.824	24.839	0.824	0.002	−2.37
P07435	Odorant-binding protein	24.827	0.703	27.250	0.703	<0.001	−2.423
F1MYY4	Interleukin-1	17.467	2.204	21.075	2.204	0.001	−3.608

[1] Protein abundance values were normalized and log2 transformed.
[2] Significant differences were considered when $P < 0.05$.
[3] Log2-transformed values were used to calculate the fold change (FC) between groups as mean (CON) - mean (PHY).

Table 4
KEGG pathways enriched in the PPI network of differentially abundant proteins regarding diet and supplementation with a phytogenic feed additive.

	#term ID	Description	Gene count	Strength	FDR[1]	Matches
Diet	bta04610	Complement and coagulation cascades	8	1.38	<0.01	*SERPINA1, SERPINC1, A2M, SERPIND1, C9, SERPING1, KNG1, C8G*
	bta04520	Adherens junction	4	1.19	0.02	*RHOA, ACTG1, RAC1,V ASP, CHAD, CAPN2, PPP1CC, VCL*
	bta05100	Bacterial invasion of epithelial cells	4	1.15	0.02	*RHOA, ACTG1, RAC1, VCL*
	bta04510	Focal adhesion	8	1.04	<0.01	*RHOA, ACTG1, RAC1, VASP, VCL*
	bta04670	Leukocyte transendothelial migration	5	1.04	0.02	*RHOA, ACTG1, RAC1, PPP1CC, KNG1, VCL*
	bta05152	Tuberculosis	6	0.91	0.02	*RHOA, ACTG1, RAC1, VCL*
	bta04810	Regulation of actin cytoskeleton	6	0.87	0.02	*RHOA, CYCS, ACTG1, RAC1, ANXA2, PYCARD*
	bta05132	Salmonella infection	6	0.85	0.02	*RHOA, CYCS, CTSD, LSP1, CATHL3, HSPD1*
Treatment	bta01210	2-Oxocarboxylic acid metabolism	3	1.38	0.02	*CS, GOT2,I DH1*
	bta00030	Pentose phosphate pathway	3	1.18	0.05	*TALDO1, PGD, G6PD*
	bta01230	Biosynthesis of amino acids	7	1.14	<0.01	*PGK1, CS, GOT2, TALDO1, ENO1, TPI1, IDH1*
	bta04610	Complement and coagulation cascades	7	1.09	<0.01	*SERPINC1, A2M, CLU, CFB, C3, F5, C4BPA*
	bta00010	Glycolysis / Gluconeogenesis	5	1.07	<0.01	*AKR1A1, PGK1, LDHA, ENO1, TPI1*
	bta00270	Cysteine and methionine metabolism	4	1.07	0.02	*GOT2, LDHA, AHCY, CCBL1*
	bta01200	Carbon metabolism	9	1.06	<0.01	*PGK1, CS, GOT2, TALDO1, ENO1, PGD, G6PD, TPI1, IDH1*
	bta00983	Drug metabolism - other enzymes	5	1	0.01	*DPYD,XDH,TPMT,CES2,NME2*
	bta05150	*Staphylococcus aureus* infection	5	0.87	0.03	*KRT15, CFB, KRT10, CATHL5, C3*
	bta04145	Phagosome	7	0.81	0.01	*THBS1, RAC1, RAB7A, CGN1, CD14, C3, TUBA3E*
	bta00230	Purine metabolism	6	0.81	0.02	*ADA, XDH, AK2, ATIC, NME2, NT5E*
	bta01100	Metabolic pathways	28	0.43	<0.01	*AKR1A1, PGK1, GYG1, CS, ADA, DPYD, GOT2, LDHA, GALNT12, NAGA, TALDO1, PYGL, XDH, ATP5B, ENO1, PGD, AK2, GALNT6, AHCY, ATIC, G6PD, TPI1, IDH1, NME2, HEXB, CCBL1, AOX4, NT5E*

[1] False discovery rate.

of microfold cells for subsequent bacteria-specific immune response against pathogenic species such as *Escherichia coli* and *Salmonella enterica* [51]. Therefore, the downregulation of this salivary protein with the change to high-concentrate diet implies a decrease in host defense capability against these potential pathogens. This is especially relevant because it indicates that the decrease in glycoprotein 2 may further increase the risk of pathogen outgrowth, already being a challenge due to drastic diet change [52].

Moreover, findings from this experiment showed increased abundance of odorant-binding proteins (Q0IIA2, P07435) when cows were supplemented with PHY. This type of proteins has been known to bind odor molecules for their transportation to the nervous systems [53].

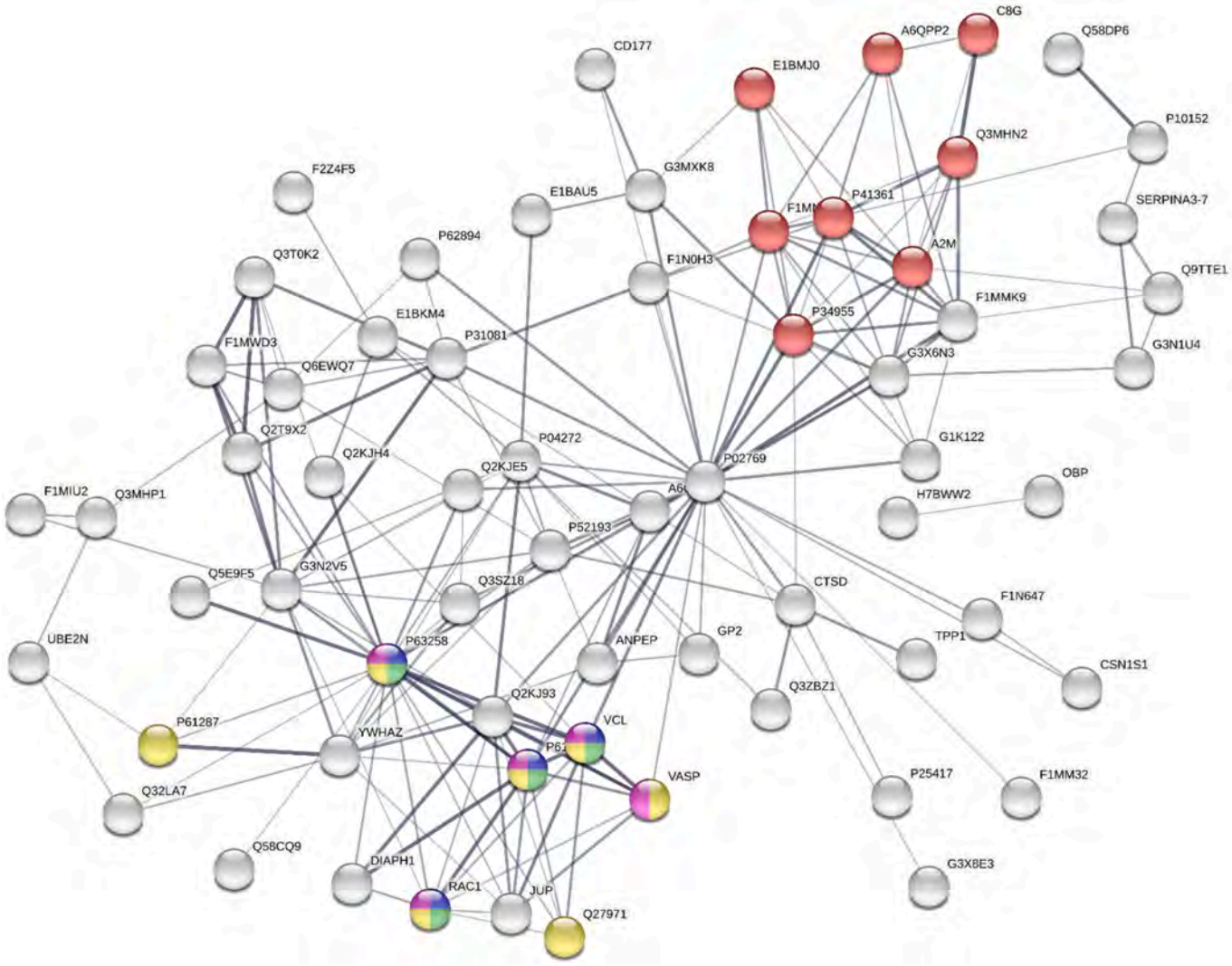

Fig. 3. PPI network of differentially abundant proteins regarding diet (red - bta04610, purple - bta04520, green - bta05100, yellow - bta04510, pink - bta04670). (For interpretation of the references to colour in this figure legend, the reader is referred to the web version of this article.)

Thus, findings reflect enhanced neural detection and recognition of the phytogenic heterocyclic compounds included in the feed supplement. Additionally, these observations support previous reports indicating that the mechanism of action of phytogenic compounds, and more specifically menthol, includes gustatory and olfactory stimulation with a direct participation of the central nervous system [54]. Therefore, these results suggest the potential of supplementation with the phytogenic feed additive to positively modulate cattle response via olfactory stimuli that can in turn influence salivary composition. Although these findings did not translate into increased feed intake, the olfactory properties of PHY may have contributed to the increased preference for dietary fiber in PHY cows, as reported in a companion paper [55]. However, more research will be needed to fully understand the effects in the host.

4.4. Salivary proteins associated with major salivary components

Our results showed that abundance of specific salivary proteins may be associated with major bioactive components of saliva, which could be linked with GO terms enriched, i.e. catalytic activity of enzymes. For example, we found that mucin-5B (F2FB42) was among the identified proteins with the highest numbers of identified peptides in the core proteome. Mucins play a crucial role in the initial stage of feed digestion because of their participation in feed bolus lubrication, which facilitates feed mastication, feed breakdown, exposure of nutrients, deglutition, and physical protection of the oral cavity [56]. Results showed that high-concentrate feeding tended to lower salivary content of total mucins. However, PHY seems to positively influence the abundance of several types of mucins, i.e. mucin-5B, suggesting beneficial effects for the animal. On the other hand, the bovine enzyme carbonic anhydrase 6 (F1MBS0) was found to be abundant in saliva. The latter finding can be explained by the involvement of this enzyme in multiple processes influencing host physiology. Specifically, carbonic anhydrase catalyses the interconversion of CO_2 and bicarbonate in parietal cells, a process involved in the formation of HCl in the abomasum. Additionally, carbonic anhydrase catalyses the hydration of CO_2 produced by oxidation of organic fuels to form bicarbonate [33]. Interestingly, salivary bicarbonate increased by 12.6% due to high-concentrate feeding. Therefore, it is possible that the decreased abundance of carbonic anhydrase 2 (F1N0H3) when cows were switched to high-concentrate reflected a response to regulate the reconversion of bicarbonate to CO_2, so that bicarbonate can be spared to buffer the ruminal pH.

Interestingly, we found that most salivary proteins correlating positively with total mucin content, correlate negatively with bicarbonate, and vice versa. The latter observation suggests pleiotropic effect of those proteins. For example, the adipogenesis regulatory factor (which has been reported in canine saliva [57]) and the CD177 molecule positively

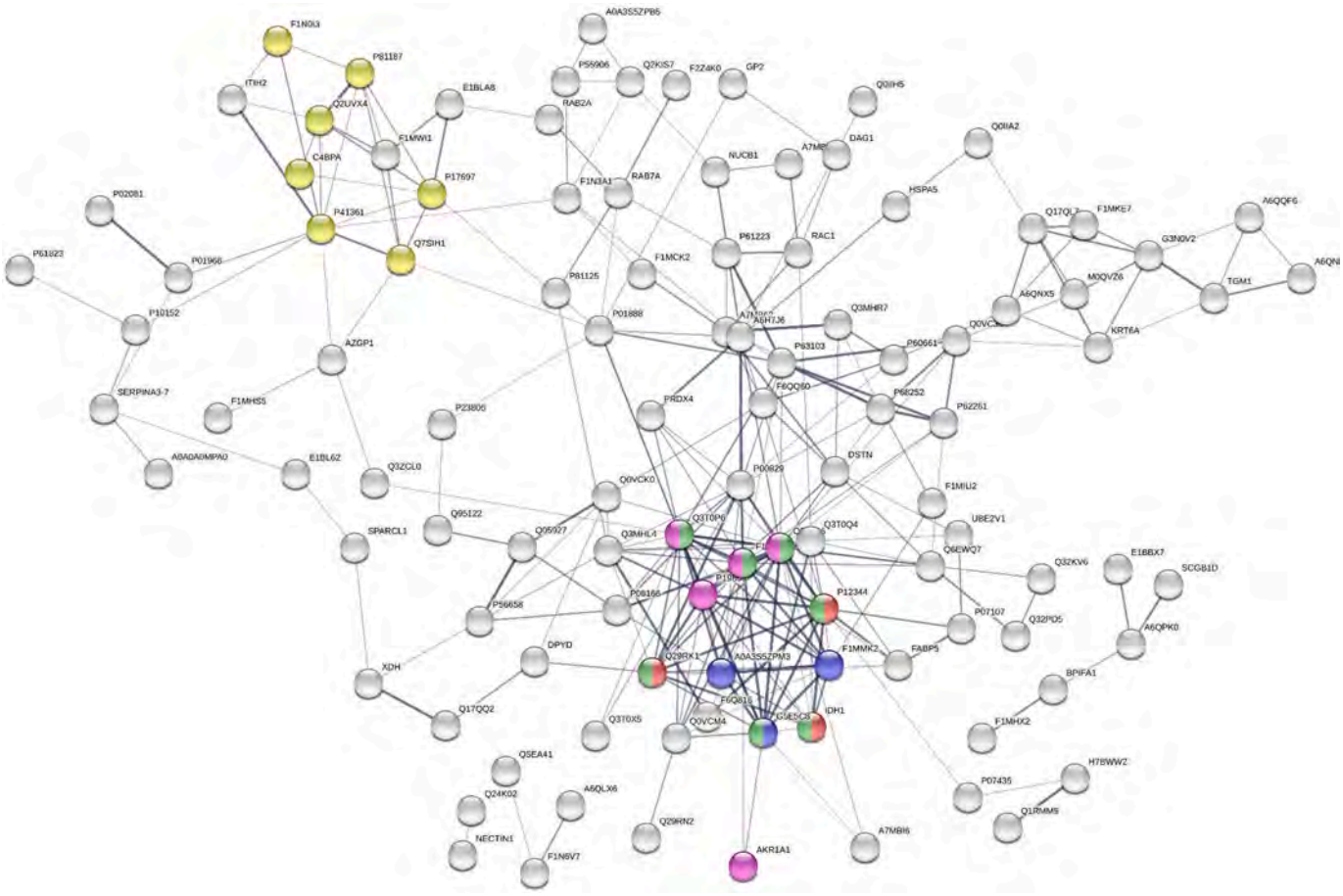

Fig. 4. PPI network of differentially abundant proteins regarding phytogenic supplementation (red - bta01210, purple - bta00030, green - bta01230, yellow - bta04610, pink - bta00010). (For interpretation of the references to colour in this figure legend, the reader is referred to the web version of this article.)

Table 5
Effects of shifting from forage to high-concentrate diet and supplementation with a phytogenic feed additive[1] on salivary physicochemical composition of dairy cows.

	Forage diet		High-concentrate diet			*P*-values[3]		
Item	CON	PHY	CON	PHY	SE[2]	D	S	I
Salivary pH	8.86	8.89	8.99	8.98	0.073	0.17	0.94	0.77
Buffer capacity, decamols HCl/L/ΔpH	0.12	0.13	0.14	0.12	0.005	0.96	0.34	0.04
Bicarbonate, mM	57.66	58.89	66.65	65.88	2.841	<0.01	0.94	0.62
Phosphate, mM	11.72	10.30	9.74	8.18	0.930	0.04	0.13	0.94
Mucins, mg/mL	2.00	1.58	1.18	1.43	0.290	0.06	0.83	0.15
Lysozyme activity, U/mL/min	27.99	34.76	26.37	30.30	6.629	0.65	0.43	0.83
Osmolality, mOsm/Kg	313.5	322.2	309.2	291.5	35.00	0.62	0.89	0.71
Total proteins, μg/mL	409.7	489.6	377.6	436.5	65.07	0.33	0.43	0.80

[1] CON: A control diet without phytogenic supplementation; PHY: supplementation with 0.04% of a phytogenic feed additive based on menthol, thymol and eugenol.
[2] The largest standard error of the mean.
[3] *P*-values for the effect of diet (D), supplementation (S) and diet × supplementation interaction (I).

correlated with bicarbonate, but negatively correlated with content of total mucins. In particular, CD177, besides its role in neutrophil activation and innate immune responses, can act as a salivary gland receptor, and has been reported to be involved in the growth and development of normal and abnormal tissue [58]. Although development of abnormal tissue in salivary glands was not expected in this study. The higher salivary bicarbonate with high-concentrate diet may also be due to changes in salivary flow rate with diet shift, as previously reported [59], because saliva flow rate influences reabsorption of salivary components in the striated duct cells [60]. Salivary tubulin beta chain protein (E1BJB1) positively correlated with mucin content in saliva. This protein is present in the microtubules of the cellular cytoskeleton [61]; thus, having a crucial role in cellular growth and structure. Therefore, the concomitant increase in the abundance of this protein and salivary mucins with diet change may reflect major changes in cells of the salivary glands involved in mucins secretion, due to increased need for feed lubrication. On the other hand, although a direct effect of interleukin-1 on salivary bicarbonate remains to be elucidated, the concomitant increase in both variables with high-concentrate feeding implies a protective response not only systemically, but also in the oral cavity given the role of bicarbonate for rising the low oral pH resulting from activity of bacterial cariogenic species.

4.5. Bacterial and plant proteins in the salivary proteome

Despite being found in relatively low proportion compared to

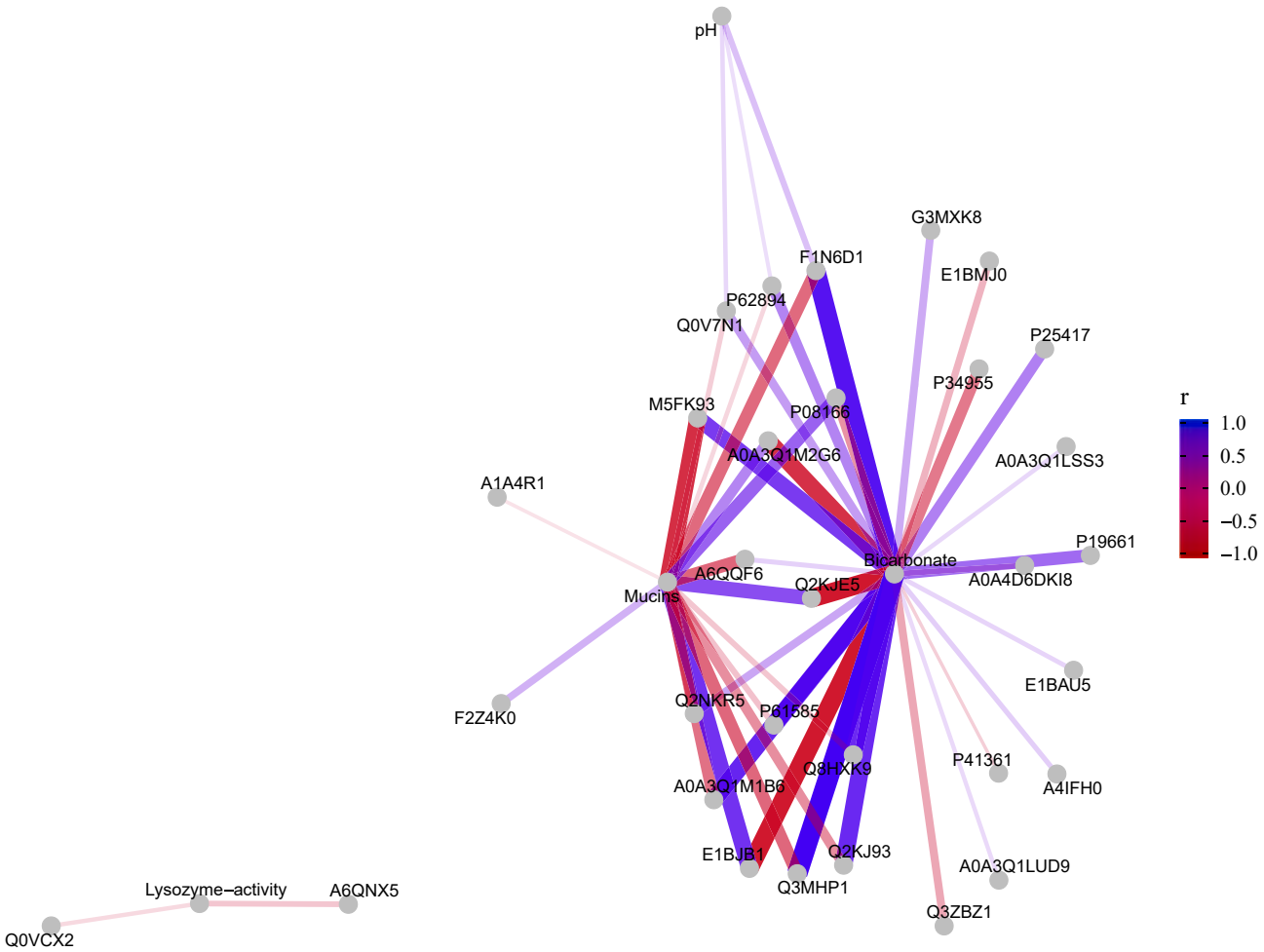

Fig. 5. Correlation network between bovine salivary physico-chemical properties and salivary proteins of bovine origin that were differentially abundant between forage and high-concentrate diets.

proteins of bovine origin, bacterial proteins detected in saliva reflect the close interplay between the animal and its gut microbiome in processes related to digestion, metabolism and supply of nutrients. Within bacterial proteins, the high abundance of polypeptides involved in bacterial protein synthesis, i.e. translation and elongation factors (P42475, Q8A463), reflects the relevance of this biomolecule representing more than half of the bacterial biomass [62]. Specifically, bacterial protein synthesis is highly important for ruminants because of its contribution to the metabolizable protein supply [63]. Furthermore, although not found within the top 10 bacterial proteins, the high abundance of the glycolytic enzyme glyceraldehyde-3-phosphate dehydrogenase (O32755) reflects the importance of the Embden-Meyerhof-Parnas pathway, one of the main routes for degradation of monomers in bacteria [64].

With regard to the effect of treatment on salivary proteins of bacterial origin, we found that animals in the CON group tended to have a higher amount of bacterial proteins in saliva. The lower number of microbial proteins found in PHY animals can be attributed to the antimicrobial properties of phytogenic compounds [65]. For example, thymol has been shown to have antimicrobial activity [66]. This is also consistent with the fact that 19 differentially abundant bacterial proteins were lower in the PHY group. Bacterial proteins that were differentially abundant between CON and PHY are elongation factors, which are closely involved in bacterial proteins synthesis and growth.

Regarding the source of oral microbes, likely some of them reached the buccal ecosystem by being transferred from forages included in the diet. For example, *Oenococcus oeni*, a lactic acid producer [67], may have proliferated during the ensiling process of corn. In addition, some of the oral bacteria originated from the ruminal microbial community due to rumination, where digesta is regurgitated, allowing movement of microbes like *Fibrobacter succinogenes* to the mouth, a highly abundant ruminal fibrolytic species [64,68]. Furthermore, certain bacterial species may have colonized the oral ecosystem because of the high availability of substrates. For example, *Akkermansia muciniphila* has been reported to degrade mucins, one of the main salivary components [69].

In this experiment, the presence of certain plant proteins in saliva was also expected. Our results are in agreement with major feed ingredients and their rate of inclusion in the diet. For example, we detected high abundance of plant proteins originating from rapeseed meal (*Brassica napus*), from barley grain (*Hordeum vulgare*), and from triticale (a hybrid of *Triticum aestivum* and *Secale cereale*) when cattle consumed the high-concentrate diet. The latter ingredients accounted for 15.5, 19.7, and 11.7%, respectively in the high-concentrate total mixed ration. Although not among the top ten plant proteins, ribulose bisphosphate carboxylase (O65194) from alfalfa (*Medicago sativa* L.) was among those with high numbers of identified peptides. This enzyme originated from grass silage (containing alfalfa), which represented 75 and 26% in the forage and high-concentrate diet, respectively. The high proportion of ribulose bisphosphate carboxylase in the salivary proteome reflects its prevalence in plants, and its importance in biological processes involving the fixation of carbon in the initial stage of the Calvin cycle during photosynthesis [33].

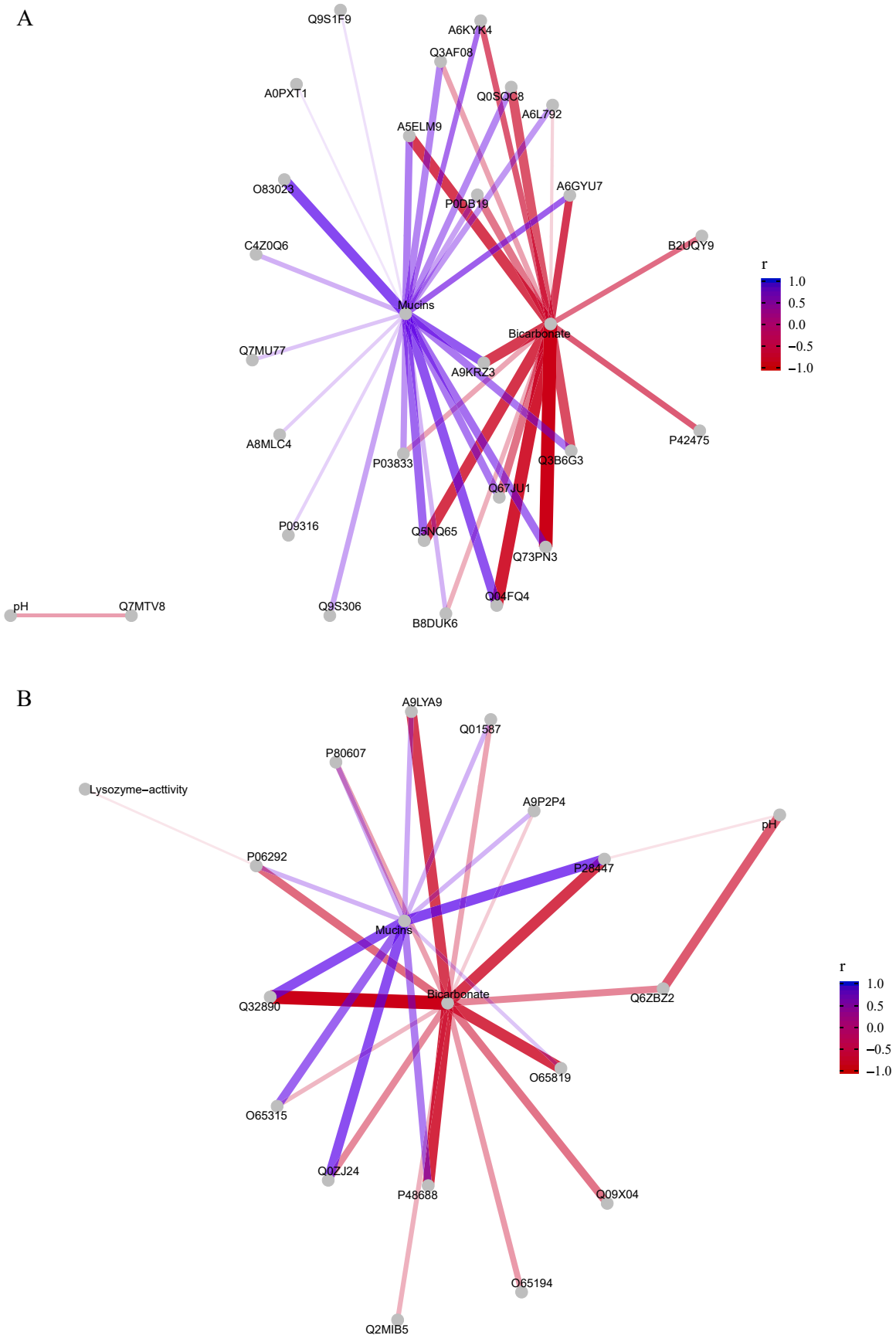

Fig. 6. Correlation network between bovine salivary physico-chemical properties and salivary proteins of bacterial (A) and plant (B) origin that were differentially abundant between forage and high-concentrate diets.

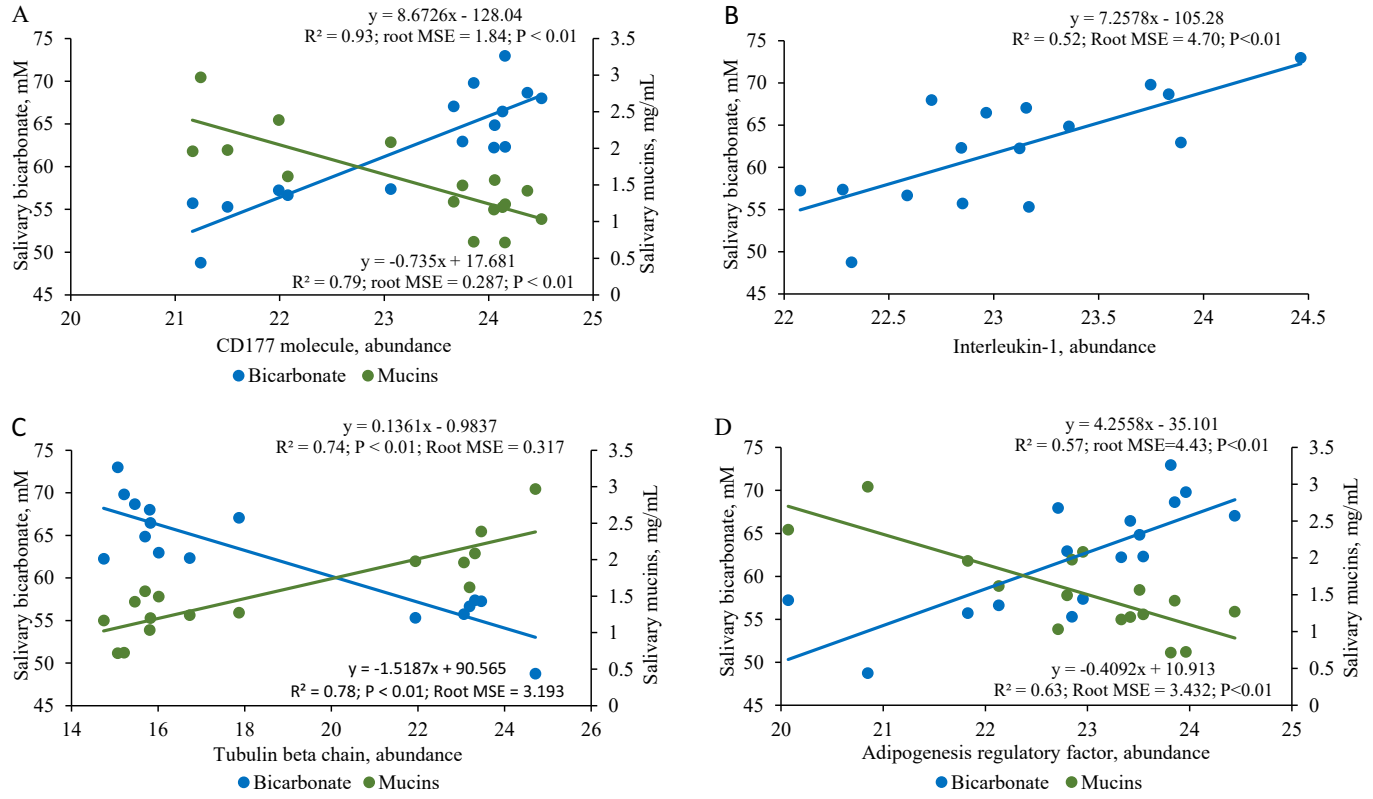

Fig. 7. Regression plots for the association of salivary proteins (CD177, A0A3Q1M1B6; A; interleukin-1, A4IFH0; B; Tubulin beta chain, E1BJB1; C; and adipogenesis regulatory factor, Q2NKR5; D) with bicarbonate as well as with total content of mucins in saliva. Protein abundance values were normalized and log2 transformed.

4.6. Limitations of the present study

A limitation of the present study may be the relatively low number of experimental units used. The analyses indicated an acceptable level of statistical power, but a greater number of animals would likely result in a more robust statistical power. Additionally, the length of this study was relatively short, and we can only make conclusions based on the evaluated timeframe. Thus, we do not know how the salivary proteome would be affected by prolonged high-concentrate feeding. Furthermore, given that we used non-lactating cows for this study, the changes observed in the salivary proteome may not be directly extrapolated to cows with a different physiological status (i.e. in lactation); thus, future research should consider the evaluation of the salivary proteome in lactating cows.

5. Conclusion

Results from the present study provide unique insights into the bovine salivary proteome, filling an important research gap in animal gut physiology. Therefore, results will have a crucial contribution for elucidating the bovine salivary proteome and to further understand animal response in terms of nutrient utilization and immune activity due a drastic change from forage to a high-energy diet, a feeding approach commonly implemented in current cattle intensive production systems worldwide. Additionally, supplementation with a phytogenic feed additive based on menthol, thymol and eugenol, increased abundance of proteins involved in smell recognition. Furthermore, findings suggest an association between specific salivary proteins and other salivary components such as bicarbonate and total mucins. Overall, findings emphasize the need of incorporating novel tools for the evaluation of cattle saliva to complement conventional analyzes of major salivary physico-chemical properties.

Funding

This work was supported by the Austrian Federal Ministry for Digital and Economic Affairs, and by the National Foundation for Research, Technology and Development (2018); and by Biomin GmbH that supports the Christian Doppler Laboratory for Innovative Gut Health Concepts of Livestock.

Data availability statement

The original contributions presented in the study are included in the article. Additional information on protein abundance data can be found at https://doi.org/10.17632/5c74mnmdb3.1, or provided as Supplementary Material. Further inquiries can be directed to the corresponding authors.

CRediT authorship contribution statement

Ezequias Castillo-Lopez: Conceptualization, Investigation, Methodology, Formal analysis, Writing - original draft. **Cátia Pacífico:** Formal analysis, Writing - original draft. **Arife Sener-Aydemir:** Methodology. **Karin Hummel:** Methodology. **Katharina Nöbauer:** Methodology. **Sara Ricci:** Investigation. **Raul Rivera-Chacon:** Investigation. **Nicole Reisinger:** Conceptualization, Funding acquisition. **Ebrahim Razzazi-Fazeli:** Methodology. **Qendrim Zebeli:** Conceptualization, Project administration, Funding acquisition. **Susanne Kreuzer-Redmer:** Conceptualization, Methodology, Formal analysis, Writing - review & editing.

Declaration of Competing Interest

Nicole Reisinger is employed by BIOMIN Holding GmbH, which is

part of DSM, a company that manufactures and trades feed additives. However, this fact did not influence the analysis of data nor the interpretation of results.

Data availability

No

Acknowledgements

We thank the staff of the dairy farm as well as laboratory technicians of the Institute of Animal Nutrition and Functional Plant Compounds of University of Veterinary Medicine Vienna for their help during the experiment. Thanks to Thomas Enzinger for helping during sample collection and to Anita Dockner for laboratory analysis.

Appendix A. Supplementary data

Supplementary data to this article can be found online at https://doi.org/10.1016/j.jprot.2022.104795.

References

[1] Amerongen A. van Nieuw, J.G.M. Bolscher, E.C.I. Veerman, Salivary proteins: protective and diagnostic value in cariology? Caries Res. 38 (3) (2004) 247–253, https://doi.org/10.1159/000077762.
[2] B.L. Schulz, J. Cooper-White, C.K. Punyadeera, Saliva proteome research: current status and future outlook, Crit. Rev. Biotechnol. 33 (3) (2013) 246–259, https://doi.org/10.3109/07388551.2012.687361.
[3] J. Wang, Y. Liang, Y. Wang, J. Cui, M. Liu, W. Du, et al., Computational prediction of human salivary proteins from blood circulation and application to diagnostic biomarker identification, PLoS One 8 (11) (2013), e80211, https://doi.org/10.1371/journal.pone.0080211.
[4] T. Pfaffe, J. Cooper-White, P. Beyerlein, K. Kostner, C. Punyadeera, Diagnostic potential of saliva: current state and future applications, Clin. Chem. 57 (5) (2011) 675–687, https://doi.org/10.1373/clinchem.2010.153767.
[5] E. Lamy, G. da Costa, F. Capela e Silva, J. Potes, A.V. Coelho, E.S. Baptista, Comparison of electrophoretic protein profiles from sheep and goat parotid saliva, J. Chem. Ecol. 34 (3) (2008) 388–397, https://doi.org/10.1007/s10886-008-9442-2.
[6] E. Lamy, M. Mau, Saliva proteomics as an emerging, non-invasive tool to study livestock physiology, nutrition and diseases, J. Proteome 75 (14) (2012) 4251–4258, https://doi.org/10.1016/j.jprot.2012.05.007.
[7] C.-S. Ang, S. Binos, M.I. Knight, P.J. Moate, B.G. Cocks, M.B. McDonagh, Global survey of the bovine salivary proteome: integrating multidimensional prefractionation, targeted, and glycocapture strategies, J. Proteome Res. 10 (11) (2011) 5059–5069, https://doi.org/10.1021/pr200516d.
[8] E. Castillo-Lopez, B.I. Wiese, S. Hendrick, J.J. McKinnon, T.A. McAllister, K. A. Beauchemin, et al., Incidence, prevalence, severity, and risk factors for ruminal acidosis in feedlot steers during backgrounding, diet transition, and finishing, J. Anim. Sci. 92 (7) (2014) 3053–3063, https://doi.org/10.2527/jas.2014-7599.
[9] Q. Zebeli, B.U. Metzler-Zebeli, Interplay between rumen digestive disorders and diet-induced inflammation in dairy cattle, Res. Vet. Sci. 93 (3) (2012) 1099–1108, https://doi.org/10.1016/j.rvsc.2012.02.004.
[10] S. Ricci, R. Rivera-Chacon, R.M. Petri, A. Sener-Aydemir, S. Sharma, N. Reisinger, et al., Supplementation with phytogenic compounds modulates salivation and salivary Physico-chemical composition in cattle fed a high-concentrate diet, Front. Physiol. 12 (2021), 645529, https://doi.org/10.3389/fphys.2021.645529.
[11] W. Yan, R. Apweiler, B.M. Balgley, P. Boontheung, J.L. Bundy, B.J. Cargile, et al., Systematic comparison of the human saliva and plasma proteomes, Proteomics Clin Appl 3 (1) (2009) 116–134, https://doi.org/10.1002/prca.200800140.
[12] L. Franco-Martínez, A. Muñoz-Prieto, M.D. Contreras-Aguilar, R. Želvytė, I. Monkevičienė, A. Horvatić, et al., Changes in saliva proteins in cows with mastitis: a proteomic approach, Res. Vet. Sci. 140 (2021) 91–99, https://doi.org/10.1016/j.rvsc.2021.08.008.
[13] G. Cobellis, M. Trabalza-Marinucci, Z. Yu, Critical evaluation of essential oils as rumen modifiers in ruminant nutrition: a review, Sci. Total Environ. 545-546 (2016) 556–568, https://doi.org/10.1016/j.scitotenv.2015.12.103.
[14] C. Benchaar, Diet supplementation with thyme oil and its main component thymol failed to favorably alter rumen fermentation, improve nutrient utilization, or enhance milk production in dairy cows, J. Dairy Sci. 104 (1) (2021) 324–336, https://doi.org/10.3168/jds.2020-18401.
[15] C. Pannitteri, M.L. Corollaro, I. Caprioli, Effectiveness of several palate cleansers on carry-over effect of minty chewing gums, Chem. Percept. 13 (2) (2020) 106–118, https://doi.org/10.1007/s12078-019-09271-x.
[16] R. Rivera-Chacon, E. Castillo-Lopez, S. Ricci, R.M. Petri, N. Reisinger, Q. Zebeli, Supplementing a phytogenic feed additive modulates the risk of subacute rumen acidosis, rumen fermentation and systemic inflammation in cattle fed Acidogenic diets, Animals 12 (9) (2022) 1201, https://doi.org/10.3390/ani12091201.
[17] E. Castillo-Lopez, R.M. Petri, S. Ricci, R. Rivera-Chacon, A. Sener-Aydemir, S. Sharma, et al., Dynamic changes in salivation, salivary composition, and rumen fermentation associated with duration of high-grain feeding in cows, J. Dairy Sci. 104 (4) (2021) 4875–4892, https://doi.org/10.3168/jds.2020-19142.
[18] R. Ruslin, M. Maskur, E. Yuliani, S.N. Depamede, Proteomics and sequence analysis of a 30-kDa saliva protein of Indonesian local goat (Capra hircus) using MALDI-TOF/TOF-MS and related techniques, Turk. J. Vet. Anim. Sci. 41 (2017) 541–547, https://doi.org/10.3906/vet-1605-57.
[19] E. Castillo-Lopez, C. Pacifico, A. Sener-Aydemir, S. Ricci, R. Rivera-Chacon, N. Reisinger, et al., The bovine salivary proteome, Mendeley data, V1, (2022), https://doi.org/10.17632/5c74mnmdb3.1.
[20] W.W. Stroup (Ed.), Mixed Model Procedures to Assess Power, Precision, and Sample Size in the Design of Experiments, 1999.
[21] P.J. Kononoff, K.J. Hanford, Technical note: estimating statistical power of mixed models used in dairy nutrition experiments, J. Dairy Sci. 89 (10) (2006) 3968–3971, https://doi.org/10.3168/jds.S0022-0302(06)72439-0.
[22] R Core Team. R, A Language and Environment for Statistical Computing, Available from: http://www.r-project.org/, 2022.
[23] X. Zhang, A.H. Smits, G.B. van Tilburg, H. Ovaa, W. Huber, M. Vermeulen, Proteome-wide identification of ubiquitin interactions using UbIA-MS, Nat. Protoc. 13 (3) (2018) 530–550, https://doi.org/10.1038/nprot.2017.147.
[24] J. Oksanen, F.G. Blanchet, R. Kindt, P. Legendre, P.R. Minchin, O'hara R., Package 'Vegan'. Community ecology package, Version 2, Available from: https://CRAN.R-project.org/package=vegan, 2022.
[25] P.D. Thomas, M.J. Campbell, A. Kejariwal, H. Mi, B. Karlak, R. Daverman, et al., PANTHER: a library of protein families and subfamilies indexed by function, Genome Res. 13 (9) (2003) 2129–2141, https://doi.org/10.1101/gr.772403.
[26] D. Szklarczyk, A.L. Gable, K.C. Nastou, D. Lyon, R. Kirsch, S. Pyysalo, et al., The STRING database in 2021: customizable protein-protein networks, and functional characterization of user-uploaded gene/measurement sets, Nucleic Acids Res. 49 (D1) (2021) D605–D612, https://doi.org/10.1093/nar/gkaa1074.
[27] K. Kishimoto, M. Nishizuka, D. Katoh, A. Kato, S. Osada, M. Imagawa, FAD104, a regulatory factor of adipogenesis, acts as a novel regulator of calvarial bone formation, J. Biol. Chem. 288 (44) (2013) 31772–31783, https://doi.org/10.1074/jbc.M113.452961.
[28] S.J. Park, S.-H. Beak, D.J.S. Jung, S.Y. Kim, I.H. Jeong, M.Y. Piao, et al., Genetic, management, and nutritional factors affecting intramuscular fat deposition in beef cattle - a review, Asian-Australas J Anim Sci 31 (7) (2018) 1043–1061, https://doi.org/10.5713/ajas.18.0310.
[29] K.J. Sonnemann, D.P. Fitzsimons, J.R. Patel, Y. Liu, M.F. Schneider, R.L. Moss, et al., Cytoplasmic gamma-actin is not required for skeletal muscle development but its absence leads to a progressive myopathy, Dev. Cell 11 (3) (2006) 387–397, https://doi.org/10.1016/j.devcel.2006.07.001.
[30] X. Zhang, X. Lin, C. Qin, K. Huang, X. Sun, L. Zhao, et al., Avian chaperonin containing TCP1 subunit 5 supports influenza a virus replication by interacting with viral nucleoprotein, PB1, and PB2 proteins, Front. Microbiol. 11 (2020), 538355, https://doi.org/10.3389/fmicb.2020.538355.
[31] J.X. Zhang, I. Braakman, K.E. Matlack, A. Helenius, Quality control in the secretory pathway: the role of calreticulin, calnexin and BiP in the retention of glycoproteins with C-terminal truncations, Mol. Biol. Cell 8 (10) (1997) 1943–1954, https://doi.org/10.1091/mbc.8.10.1943.
[32] F.U. Hartl, A. Bracher, M. Hayer-Hartl, Molecular chaperones in protein folding and proteostasis, Nature 475 (7356) (2011) 324–332, https://doi.org/10.1038/nature10317.
[33] A.L. Lehninger, D.L. Nelson, M.M. Cox, Lehninger Principles of Biochemistry, 4th ed., W.H. Freeman, New York, N.Y., Basingstoke, 2005.
[34] S. Asahara, Y. Shibutani, K. Teruyama, H.Y. Inoue, Y. Kawada, H. Etoh, et al., Ras-related C3 botulinum toxin substrate 1 (RAC1) regulates glucose-stimulated insulin secretion via modulation of F-actin, Diabetologia 56 (5) (2013) 1088–1097, https://doi.org/10.1007/s00125-013-2849-5.
[35] C. Pacífico, S. Ricci, F. Sajovitz, E. Castillo-Lopez, R. Rivera-Chacon, R.M. Petri, et al., Bovine rumen epithelial miRNA-mRNA dynamics reveals post-transcriptional regulation of gene expression upon transition to high-grain feeding and phytogenic supplementation, Genomics 114 (3) (2022), 110333, https://doi.org/10.1016/j.ygeno.2022.110333.
[36] X. Wei, X. Liu, C. Tan, L. Mo, H. Wang, X. Peng, et al., Expression and function of zinc-α2-glycoprotein, Neurosci. Bull. 35 (3) (2019) 540–550, https://doi.org/10.1007/s12264-018-00332-x.
[37] F.N. Owens, D.S. Secrist, W.J. Hill, D.R. Gill, Acidosis in cattle: a review, J. Anim. Sci. 76 (1) (1998) 275–286, https://doi.org/10.2527/1998.761275x.
[38] C. Bárcena, M. Stefanovic, A. Tutusaus, G.A. Martinez-Nieto, L. Martinez, C. García-Ruiz, et al., Angiogenin secretion from hepatoma cells activates hepatic stellate cells to amplify a self-sustained cycle promoting liver cancer, Sci. Rep. 5 (2015) 7916, https://doi.org/10.1038/srep07916.
[39] E. Castillo-Lopez, R. Rivera-Chacon, S. Ricci, N. Reisinger, Q. Zebeli, Changes in fermentation profile of the reticulorumen and hindgut, and nutrient digestion in dry cows fed concentrate-rich diets supplemented with a phytogenic feed additive, J. Dairy Sci. 105 (7) (2022) 5747–5760, https://doi.org/10.3168/jds.2022-21786.
[40] G. Dickneite, B. Leithäuser, Influence of antithrombin III on coagulation and inflammation in porcine septic shock, Arterioscler. Thromb. Vasc. Biol. 19 (6) (1999) 1566–1572, https://doi.org/10.1161/01.ATV.19.6.1566.
[41] J.G. Lees, Y.W. Ching, D.H. Adams, C.T.T. Bach, M.S. Samuel, A.J. Kee, et al., Tropomyosin regulates cell migration during skin wound healing, J Invest Dermatol 133 (5) (2013) 1330–1339, https://doi.org/10.1038/jid.2012.489.

[42] S.B. Marston, C.S. Redwood, The essential role of tropomyosin in cooperative regulation of smooth muscle thin filament activity by caldesmon, J. Biol. Chem. 268 (17) (1993) 12317–12320, https://doi.org/10.1016/s0021-9258(18)31391-7.
[43] P. Scocco, F. Mercati, F.M. Tardella, A. Catorci, Increase of forage dryness induces differentiated anatomical response in the sheep rumen compartments, Microsc. Res. Tech. 79 (8) (2016) 738–743, https://doi.org/10.1002/jemt.22692.
[44] Benedeti P. Del Bianco, BdC Silva, M.V.C. Pacheco, N.V.L. Serão, I. Carvalho Filho, M.M. Lopes, et al., Effects of grain processing methods on the expression of genes involved in volatile fatty acid transport and pH regulation, and keratinization in rumen epithelium of beef cattle, PLoS One 13 (6) (2018), e0198963, https://doi.org/10.1371/journal.pone.0198963.
[45] K. Hodge, S.T. Have, L. Hutton, A.I. Lamond, Cleaning up the masses: exclusion lists to reduce contamination with HPLC-MS/MS, J. Proteome 88 (2013) 92–103, https://doi.org/10.1016/j.jprot.2013.02.023.
[46] T.G. Nagaraja, M.M. Chengappa, Liver abscesses in feedlot cattle: a review, J. Anim. Sci. 76 (1) (1998) 287–298, https://doi.org/10.2527/1998.761287x.
[47] M. Hoge, S. Amar, Role of interleukin-1 in bacterial atherogenesis, Drugs Today (Barc) 42 (10) (2006) 683–688, https://doi.org/10.1358/dot.2006.42.10.1003543.
[48] A. Lavagna, J.-P. Auger, A. Dumesnil, D. Roy, S.E. Girardin, N. Gisch, et al., Interleukin-1 signaling induced by Streptococcus suis serotype 2 is strain-dependent and contributes to bacterial clearance and inflammation during systemic disease in a mouse model of infection, Vet. Res. 50 (1) (2019) 52, https://doi.org/10.1186/s13567-019-0670-y.
[49] D.F. Stroncek, L. Caruccio, M. Bettinotti, CD177: a member of the Ly-6 gene superfamily involved with neutrophil proliferation and polycythemia vera, J. Transl. Med. 2 (1) (2004) 8, https://doi.org/10.1186/1479-5876-2-8.
[50] H. Turula, C.E. Wobus, The role of the polymeric immunoglobulin receptor and secretory immunoglobulins during mucosal infection and immunity, Viruses 10 (5) (2018), https://doi.org/10.3390/v10050237.
[51] H. Ohno, K. Hase, Glycoprotein 2 (GP2): grabbing the FimH bacteria into M cells for mucosal immunity, Gut Microbes 1 (6) (2010) 407–410, https://doi.org/10.4161/gmic.1.6.14078.
[52] M.E. Jacob, J.T. Fox, J.S. Drouillard, D.G. Renter, T.G. Nagaraja, Effects of dried distillers' grain on fecal prevalence and growth of Escherichia coli O157 in batch culture fermentations from cattle, Appl. Environ. Microbiol. 74 (1) (2008) 38–43, https://doi.org/10.1128/AEM.01842-07.
[53] P. Pelosi, Odorant-binding proteins, Crit. Rev. Biochem. Mol. Biol. 29 (3) (1994) 199–228, https://doi.org/10.3109/10409239409086801.
[54] D.D. McKemy, The molecular and cellular basis of cold sensation, ACS Chem. Neurosci. 4 (2) (2013) 238–247, https://doi.org/10.1021/cn300193h.
[55] R. Rivera-Chacon, S. Ricci, R.M. Petri, A. Haselmann, N. Reisinger, Q. Zebeli, et al., Effect of duration of high-grain feeding on chewing, feeding behavior, and salivary composition in cows with or without a phytogenic feed supplement, Animals (Basel) 12 (15) (2022), https://doi.org/10.3390/ani12152001.
[56] L.A. Tabak, M.J. Levine, I.D. Mandel, S.A. Ellison, Role of salivary mucins in the protection of the oral cavity, J Oral Pathol 11 (1) (1982) 1–17, https://doi.org/10.1111/j.1600-0714.1982.tb00138.x.
[57] L. Franco-Martínez, A. Gelemanović, A. Horvatić, M.D. Contreras-Aguilar, R. Dąbrowski, V. Mrljak, et al., Changes in serum and salivary proteins in canine mammary tumors, Animals (Basel) 10 (4) (2020), https://doi.org/10.3390/ani10040741.
[58] D. Andreadis, A. Epivatianos, A. Poulopoulos, A. Nomikos, G. Papazoglou, D. Antoniades, et al., Detection of C-KIT (CD117) molecule in benign and malignant salivary gland tumours, Oral Oncol. 42 (1) (2006) 57–65, https://doi.org/10.1016/j.oraloncology.2005.06.014.
[59] G.E. Chibisa, K.A. Beauchemin, G.B. Penner, Relative contribution of ruminal buffering systems to pH regulation in feedlot cattle fed either low- or high-forage diets, Animal 10 (7) (2016) 1164–1172, https://doi.org/10.1017/S1751731115002888.
[60] H.M. Sommer, D. Kaiser, E. Drack, pH and bicarbonate excretion in the rat parotid gland as a function of salivary rate, Pflugers Arch. 355 (4) (1975) 353–360, https://doi.org/10.1007/BF00579856.
[61] P. Zuccotti, D. Cartelli, M. Stroppi, V. Pandini, M. Venturin, A. Aliverti, et al., Centaurin-α$_2$ interacts with β-tubulin and stabilizes microtubules, PLoS One 7 (12) (2012), e52867, https://doi.org/10.1371/journal.pone.0052867.
[62] E. Storm, E.R. Orskov, The nutritive value of rumen micro-organisms in ruminants. 4. The limiting amino acids of microbial protein in growing sheep determined by a new approach, Br. J. Nutr. 52 (3) (1984) 613–620, https://doi.org/10.1079/bjn19840128.
[63] E.C. Schwab, C.G. Schwab, R.D. Shaver, C.L. Girard, D.E. Putnam, N. L. Whitehouse, Dietary forage and nonfiber carbohydrate contents influence B-vitamin intake, duodenal flow, and apparent ruminal synthesis in lactating dairy cows, J. Dairy Sci. 89 (1) (2006) 174–187, https://doi.org/10.3168/jds.S0022-0302(06)72082-3.
[64] J.B. Russell, Rumen Microbiology and its Role in Ruminant Nutrition, Cornell University, College of Agriculture and Life Sciences, Ithaca NY, 2002.
[65] C. Yang, M.A.K. Chowdhury, Y. Huo, J. Gong, Phytogenic compounds as alternatives to in-feed antibiotics: potentials and challenges in application, Pathogens 4 (1) (2015) 137–156, https://doi.org/10.3390/pathogens4010137.
[66] B.J. Juven, J. Kanner, F. Schved, H. Weisslowicz, Factors that interact with the antibacterial action of thyme essential oil and its active constituents, J Appl Bacteriol 76 (6) (1994) 626–631, https://doi.org/10.1111/j.1365-2672.1994.tb01661.x.
[67] M.P. Lorentzen, H. Campbell-Sills, T.S. Jorgensen, T.K. Nielsen, M. Coton, E. Coton, et al., Expanding the biodiversity of Oenococcus oeni through comparative genomics of apple cider and kombucha strains, BMC Genomics 20 (1) (2019) 330, https://doi.org/10.1186/s12864-019-5692-3.
[68] S. Kittelmann, M.R. Kirk, A. Jonker, A. McCulloch, P.H. Janssen, Buccal swabbing as a noninvasive method to determine bacterial, archaeal, and eukaryotic microbial community structures in the rumen, Appl. Environ. Microbiol. 81 (21) (2015) 7470–7483, https://doi.org/10.1128/AEM.02385-15.
[69] M. Derrien, M.C. Collado, K. Ben-Amor, S. Salminen, W.M. Vos, The mucin degrader Akkermansia muciniphila is an abundant resident of the human intestinal tract, Appl. Environ. Microbiol. 74 (5) (2008) 1646–1648, https://doi.org/10.1128/AEM.01226-07.